UNIVERSIDADE DE LISBOA
FACULDADE DE CIÊNCIAS
DEPARTAMENTO DE FÍSICA

Computer Aided Method for 3D Assessment of the Lower Limb Alignment for Orthopedic Surgery Planning

Tomás Augusto Esteves Ferreira

Mestrado Integrado em Engenharia Biomédica e Biofísica
Perfil em Engenharia Clínica e Instrumentação Médica

Dissertação orientada por:
Prof. Doutor Hugo Alexandre Ferreira, Faculdade de Ciências
Jalil Jalal, M.Sc., Technical University of Munich

2017

ACKNOWLEDGEMENTS

I would like to start by thanking both my supervisors, Hugo Ferreira and Jalil Jalali, for their support and encouragement, their valuable advice and guidance and also for their friendliness trough all my time as their student. Both of them are excellent professionals and I was lucky to have them as my teachers and supervisors.

I would also like to thank Dr. Julian Fürmetz for teaching me and guiding me trough all the medical aspect of my work and for always being more than helpful.

Completing this work would have been a lot more difficult were it not for my coworkers at the CAPS group: thank you Christina for all the time you spent explaining me everything I needed and for always being availabe to help me with anything; Thank you Andreas for showing me how to proper segment with all your skill and for giving my days a good dose of fun; and thank you Thekla for keeping me company at the office day after day, hearing my problems and, most of all, for being my friend! Vielen Danke!

I would also like to express my deep gratitude to my family, for trusting me, believing in me and encouraging me to always follow my dreams and to always to my best. None of this would have been possible without you and I hope this work makes you proud!

Also, a big thank you to all my friends. My academic experience would have been a total different thing without you. We laughed together, we had fun together, but also worked a lot together, and all your support throughout the years is something I will never forget.

Finally, I would like to thank the Erasmus+ program for enabling this amazing experience.

RESUMO

Os membros inferiores são responsáveis por fornecer suporte à totalidade do corpo humano e são essenciais nas mais variadas tarefas como estar de pé, andar e correr. Por vezes, e devido a diversos motivos, podem existir defeitos ou deformações nos membros inferiores que têm um impacto direto na qualidade de vida de uma pessoa, quer por se ver afetado o lado estético pessoal ou por condicionar significativamente a mobilidade. Uma característica da estrutura do membro inferior que é diretamente afetada por estas deformações é o seu alinhamento, isto é, a posição relativa dos ossos e articulações que compõem o membro. Graças à evolução da medicina moderna, corrigir estas deformações é agora uma prática bastante comum no campo da cirurgia ortopédica. No entanto, antes de qualquer cirurgia corretiva e até de qualquer planeamento que esta exija, a deformação tem de ser corretamente analisada, o que é feito através da chamada avaliação do alinhamento do membro inferior. Atualmente, num contexto clínico, esta avaliação é feita manualmente num espaço de trabalho bi-dimensional, normalmente utilizando apenas imagens de raios-X da perna inteira no plano anatómico frontal.

Uma revisão ao estado da arte no que toca a métodos de planeamento cirúrgico dedicados ao membro inferior permite concluir que de facto existe software capaz de realizar este planeamento, mas que, no entanto, para além de terem custos elevadíssimos associados, nenhum utilizada modelos 3D como fonte de informação, o que traria imensos benefícios, especialmente ao nível da informação acerca da rotação e da inclinação dos ossos. Existem no entanto algum software a um nível mais experimental que utiliza modelos 3D para realizar a avaliação do alinhamento do membro inferior, sendo que nenhum deles passou ainda a estar disponível comercialmente.

Numa perspetiva de implementar um método automático baseado em computador para realizar o planeamento pré-cirurgico da cirurgia de correção para ser utilizado em contexto clínico, foi proposto um projeto para o desenvolvimento de um novo software capaz de efetuar a avaliação do alinhamento do membro inferior em modelos 3D dos doentes. O projeto foi dividido em quatro etapas distintas que se desenrolaram ao longo de um estágio de sete meses.

Na primeira etapa, o objetivo consistiu em gerar diversos modelos 3D dos membros inferiores de diferentes pacientes. Para tal, recorreu-se ao software de segmentação de imagens médicas *Mimics 14.0* e utilizaram-se imagens de tomografia computorizada dos pacientes. Após o processo de segmentação, obtiveram-se os modelos 3D cuja qualidade teve de ser assegurada através de um processo de remeshing e cuja correta orientação espacial teve de ser também assegurada, já que a avaliação do alinhamento é sensível à orientação da perna. Para tal, utilizou-se o software de renderização 3D *Geomagic Studio 14*. Optou-se ainda por separar os modelos dos ossos nas suas porções proximal e distal, de modo a reduzir futuramente os tempos de computação. Findo todo este

processo, assegurou-se que diferentes utilizadores poderiam gerar estes modelos sem grande variabilidade ou erro no resultado final através da comparação dos modelos obtidos de um mesmo paciente por três utilizadores distintos, sendo que os modelos obtidos apresentavam volumes com diferenças inferiores a 1% relativamente ao valor médio e com um baixo desvio padrão.

Numa segunda etapa, os ângulos e medidas consideradas necessárias para uma avaliação adequada foram definidos, apresentando os valores esperados para estas medidas de acordo com a literatura. Assim, foi possível definir também os pontos anatómicos que são necessários para a definição destes mesmos ângulos e medidas e que portanto têm de ser encontrados pelo software.

Na terceira etapa, fez-se então o desenvolvimento propriamente dito do software. Encontravam-se já disponíveis alguns métodos automáticos desenvolvidos no contexto projeto, contudo, estes métodos exigiam que o utilizador conhecesse as ferramentas do Geomagic de modo a obter algumas informações, e que depois fosse capaz de utilizar estas informações para editar os scripts de modo a que estes funcionassem para cada paciente em específico. Para além disso, apenas pontos muito específicos podiam ser encontrados. Nesse sentido, isto é, de modo a que todo o processo de encontrar os pontos anatómicos relevantes pudesse ser feito diretamente pelo utilizador, no programa, e sem exigir quaisquer conhecimentos de programação, um conjunto de técnicas foi implementado, dando ao programa uma grande componente gráfica.

Para os diferentes pontos, foi necessário recorrer a diferentes metodologias, algumas desenvolvidas propositadamente para o efeito e implementadas em linguagem de programação *Python* "pura", e algumas adaptadas de outras já existentes e disponíveis no próprio Geomagic. Foi ainda assegurado que existiam métodos alternativos caso os métodos padrão não fossem os mais adequados devido a uma estrutura diferente da esperada dos próprios modelos 3D.

De todo este processo resultou um programa que usa os modelos 3D gerados e, da maneira mais automática possível e com uma interface do utilizador fácil de usar, fornece todos os ângulos e medidas, efetuando assim a dita avaliação do alinhamento do membro inferior em 3D.

Uma análise ponderada aos resultados obtidos permitiu identificar quais os pontos anatómicos que estarão a ser obtidos de maneira menos ideal e por isso a levar a alguns resultados não tão bons como o esperado. A dependência criada da seleção e limitação de certas áreas nas quais ocorre uma iteração que permite encontrar certos pontos é possivelmente a maior falha do programa desenvolvido que se torna assim demasiado sensível ao input do utilizador. Note-se, contudo, que os próprios testes apresentam algumas falhas que podem influenciar os resultados obtidos, tal como não ter sido definido um roteiro de teste que obrigasse a uma utilização uniforme por parte de todos os utilizadores, e também os diferentes níveis de experiência com o programa por parte dos utilizadores de teste.

No entanto, a maioria das medidas obtidas apresenta valores constantes ao longo de diversas utilizações, igualando os valores que seriam obtidos manualmente, mas com o potencial de os obter em metade do tempo. Pode concluir-se então que, no momento, a avaliação do alinhamento 3D é possível utilizando o software desenvolvido.

É possível ainda apontar algumas limitações e fazer algumas sugestões de modo a que estas sejas ultrapassadas. Algumas limitações partiram do facto da experiência a programar em *Python* ser bastante limitada, e outras partiram do software utilizado para fazer o desenvolvimento. Por exemplo, o método que teria sido o mais indicado para encontrar um certo número de pontos na Tibia não foi possível de implementar devido a um bug interno do software.

Existe ainda muita coisa que pode ser feita no que toca ao software desenvolvido e ao objetivo final de desenvolver um método de planeamento pré-operativo: em primeiro lugar, é necessário realizar mais testes, de modo a aumentar o tamanho da amostra e o intervalo de confiança dos testes; em segundo lugar, eliminar a dependência do *Geomagic* para utilizar o programa seria o ideal; finalmente, de modo a completar o plano inicial, deve ser implementada a possibilidade de visualizar o resultado da cirurgia nos modelos 3D.

Palavras-chave: Alinhamento do Membro Inferior; Avaliação 3D do Alinhamento; Software Planeamento Pré-Cirúrgico; Planeamento de Correção de Deformações;

ABSTRACT

The lower limbs are responsible for supporting the body and are essential for several tasks such as standing, walking and running. Sometimes, and due to various reasons, defects or deformities can be found on the lower limbs and this has an impact on a person's quality-of-life. One characteristic of the structure of the lower limb that is affected by these deformities is its alignment, i.e. the relative positions of the bones and joints that it includes. Thanks to the evolution of modern medicine, fixing these deformities is now a common practice in the orthopedics' surgical field. Before any corrective surgery and its respective planning, the deformity needs to be properly analyzed, which is accomplished by the assessment of the alignment of the whole lower limb. Currently, in clinical setting, this assessment is carried out manually in the two-dimensional space, normally using whole-leg X-ray images of the anatomical frontal plane, but complex deformities can not be assessed properly in a 2D image.

In a desire to create an automatic computer-based method for the preoperative planning of deformity correction and knee surgery, a project consisting of developing a new software for assessing the lower limb alignment based on 3D models was proposed. The project was comprised of four stages: In the first stage, 3D models of different patients' lower limbs were generated using both segmentation and 3D rendering software, and it was ensured that these models could be generated by any user without significant variability/error in the final outcome; In the second stage, the exact angles and measures needed for a proper assessment were defined, as well as the anatomic landmarks required to calculate them that should then be found by the software; During the third stage, the software development took place, from which resulted a program that uses the generated 3D models and, in the most automatic way possible and with an easy-to-use interface, returns all the needed angles and measures; The final stage of the project was to ensure that the program is reliable and consistent in its results in both intraobserver and interobserver domain, and that it composes an improvement when compared with the manual procedure, while also ensuring that the results obtained by using the program match those obtained manually.

A lot can still be done and improved regarding the developed software and the ultimate goal of fully developing a preoperative planning method, but, so far, the 3D alignment assessment that results from the program has been considered to perform its task properly and in an improved way when compared to the traditional technique, even though some limitations can be observed.

Keywords: Lower Limb Alignment; 3D Alignment Assessment; Computer-based Preoperative Planning; Deformity Correction Planning;

TABLE OF CONTENTS

List of Figures

LIST OF TABLES

List of Abbreviations

CAPS	Computer Aided Plastic Surgery
LMU	Ludwig-Maximillian University
MAD	Mechanical Axis Deviation
CORA	Center of Rotation of Angulation
ACA	Angulation Correction Axis
3D	Three-Dimensional
CT	Computed Tomography
MRI	Magnetic Resonance Imaging
2D	Two-Dimensional
BPR	Biplanar Radiography
FTA	Femur Torsion Angle
HKA	Hip-Knee-Ankle Angle
TTA	Tibia Torsion Angle
M.A.D.	Mean Absolute Deviation
LPTA	Lateral Proximal Femoral Angle
mLDFA	(Mechanical) Lateral Distal Femoral Angle
MPTA	Medial Proximal Tibia Angle
MPFA	Medial Proximal Femur Angle
CCD	Centrum-Collum-Diaphysis Angle

1. INTRODUCTION

The research group CAPS - Computer Aided Plastic Surgery - from the *Klinikum Rechts der Isar* of the Technical University of Munich (TUM), and the *3D Chirurgie* group from the *Klinik für Allgemeine, Unfall- und Wiederherstellungschirurgie* of the Ludwig-Maximillian University (LMU), also located in Munich, plan to develop a novel method for the preoperative planning of deformity correction and knee surgery to be used in a real-life clinical context.

As a starting point, a project consisting of developing and validating a new software for assessing the lower limb alignment based on three-dimensional (3D) models of patients' bones, was proposed and carried out during a 7-months internship. The stages, results and outcome analysis of this project/internship are presented in this thesis over the following chapters.

In Chapter 2, some background information is exposed in order to familiarize the reader with some concepts and also to introduce the need for the work developed. In Chapter 3, the state-of-the-art relevant to this work is explored. Chapter 4 then presents the motivation for this work and the specific objectives that were proposed. The next chapters address these objectives: Chapter 5 focuses on the generation of patient's 3D models, Chapter 6 explores the design of the alignment assessment program and Chapter 7 focuses on testing the program. In Chapter 8, the limitations of the development process are discussed. Chapter 9 offers a perspective on possible future work. Finally, Chapter 10 serves as the conclusion of this work.

2. BACKGROUND

This chapter aims to introduce basic concepts on lower limb deformities and respective corrective orthopedic surgery. A particular interest is put on the need for better, more precise, surgery planning techniques.

2.1. LOWER LIMB ALIGNMENT

The lower limb, or lower extremity, of the human body can be defined in a more rigorous, human anatomical way, or in the general sense. While the first refers to the lower limb as extending from the knee to the ankle, the second way of defining it includes the entire lower extremity of the human body, which includes the foot, thigh (the portion between hip and knee) and even the hip. The common usage is followed.

The lower limbs are responsible for supporting the body and are essential for standing, walking and running, among other things. Therefore, the structure of the lower limb reflects its function in body support and movement, and changes to this structure have direct consequences on how primary functions are executed, ultimately damaging a person's quality of life.[1]

One characteristic of the structure of the lower limb is its alignment, i.e. the relative positions of the bones and joints that it includes.

2.1.1. STRUCTURE OF THE LOWER LIMB

Each lower extremity has 30 bones. The major bones of the lower limb are the Femur, Tibia and Fibula.[1] These bones are the ones considered relevant for the rest of the work. The Patella, also a major bone, is the bone in front of the knee. They can be seen in Figure 2.1.

The Femur, the most proximal bone of the three, is the longest and strongest bone in the body, being easily identified for its prominent and round head, part of the hip joint, its well defined neck and its two condyles (rounded protuberances). Worth mentioning are also the two trochanters (also bony protuberances, but not rounded) on the upper extremity and the intercondylar fossa/notch of the Femur between the two condyles.[1]

The Tibia, the second largest bone in the body, connects the knee with the ankle bones and it can be characterized by its two slightly concave condyles on the proximal end and the intercondylar eminence, forming the tibial plateau, a critical weight-bearing area which articulates with the Femur; and by the medial malleolus, which is part of the ankle joint.[1]

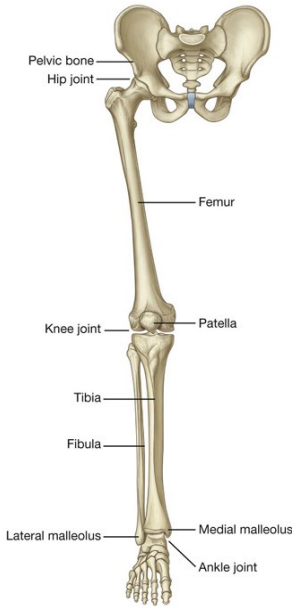

Figure 2.1 Major bones, anatomical landmarks and joints of the lower limb (from [A]).

Finally, the Fibula is the smallest and slenderest of the three bones, having a small upper extremity, placed toward the back of the head of the Tibia and below the knee joint, and a lower extremity, the lateral malleolus, which is also part of the ankle joint.[1]

Normally, the large joints of the lower limb are aligned on a straight line, which is the mechanical longitudinal axis of the leg (also identified as the Mikulicz line). This line stretches from the hip joint, through the knee joint and down to the center of the ankle, as can be seen in Figure 2.2. The distance between the mechanical axis of the lower limb and the center of the knee joint is called the Mechanical Axis Deviation (usually identified as MAD).[2]

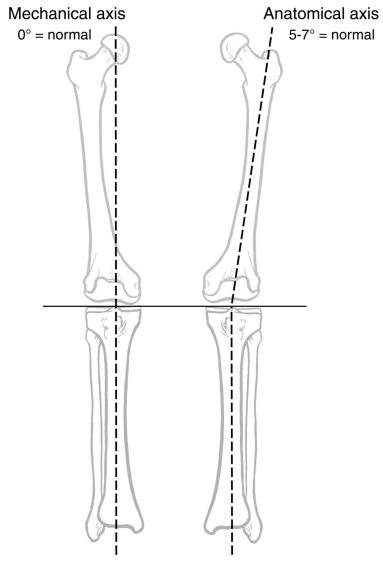

Figure 2.2. Mechanical and anatomical axis of the lower limb (from [B])

2.1.2. DEFORMITIES

Sometimes, defects or deformities can be found on the lower limb and this can be due to many different causes. These defects are congenital (present at birth), causing alterations in the shape and appearance of the legs, and sometimes the deformities may occur at a later stage as a result of trauma.

The exact cause of the congenital deformities is not known. There are several factors such as genetic factors which influence the fetal growth in the womb and drugs that can cause congenital deformities. Also, a fetus' position in the womb or vitamin/nutrition deficiencies in its development might also play a role in the formation of these deformities.[3]

The most common malformations, or malalignments, of the lower limb result from an axial deviation in the frontal plane: it is a case of genu varum (or Varus Deformity) if the mechanical axis is medial to the center of the knee joint, or of genu valgum (or Valgus Deformity) if the mechanical axis is lateral to the center of the knee joint.[2] These deformations can be observed in Figure 2.3.

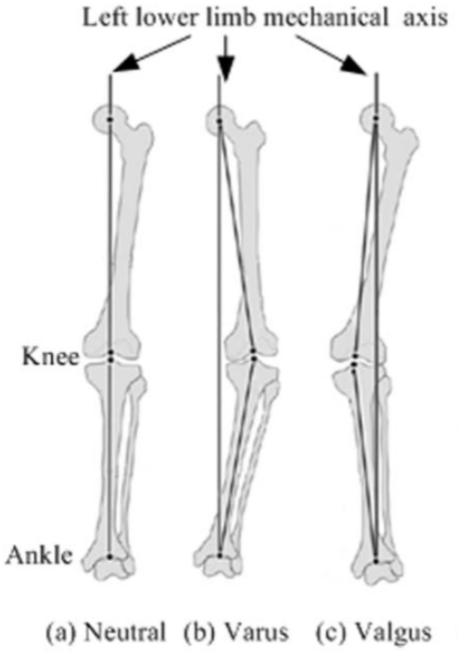

Figure 2.3. Mechanical Axis of the Lower Limb on normal and deformed lower limbs (from [C]).

These deformities have an impact on a person's quality-of-life, either by affecting the general aesthetic of the body or by affecting the mobility. They lead to unphysiological stresses on the affected joints and can thus cause pain and damage to the joint, so diseases such as arthrosis may arise as a consequence. In account of the possible consequences, it is normal that techniques have been developed in the surgical field that are capable of fixing these problems.

2.2. MALALIGNMENT/DEFORMITY CORRECTION

Thanks to the evolution of modern medicine, fixing the deformities in the lower limb is now a common practice in the orthopedics' surgical field. Some deformities are easier to fix than others, but

they all require a very specific and personalized surgery planning in order to perform the needed corrections successfully and with as high a precision as possible.

2.2.1. Deformity Analysis/Alignment Assessment Overview

Before any corrective surgery and its respective planning, the deformity needs to be properly analyzed, i.e. the alignment of the lower limb needs to be assessed.

Varus and Valgus deformities can occur both on the Femur and Tibia, which lead to a MAD outside its normal range. To determine whether MAD results from a femoral or tibial deformity, the mechanical joint orientation angles of both Femur and Tibia are measured and compared with the normal acceptable range (85º–90º). Obtained values outside of this normal range indicate the source of MAD to be femoral, tibial, or both. Performing this comparison is what is called doing a malalignment test.[4]

These deformities also affect the normal value of the femorotibial angle, and measurements can also be performed to access its value and compare it to the normal acceptable range.

The intersection point of the proximal and distal anatomical axes lines of a deformed bone is the Center Of Rotation of Angulation (usually identified as CORA). Since a change in the axes and joint angles is possible in all three planes, extremely complex dislocations can be found with simultaneous deviation of several parameters, making the identification of the CORA harder.[4]

Once the source of the deformity is identified as being femoral, tibial or both (by using the MAD or the femorotibial angle), the CORA can be found on the corresponding bone (or considering both bones, if that is the case).

Finding other angle values, e.g. in the sagittal or axial plane, that are out of normal range will also have an impact on what corrections need to be planned.

Currently, the alignment assessment is carried out manually in the two-dimensional space, normally using whole-leg X-ray images of the anatomical frontal plane. Deviations in the sagittal plane can be determined with lateral X-ray images and in the transversal plane via the evaluation of axial computed tomographic images.

2.2.2. Surgery and Planning Overview

Osteotomy literally means “cutting of a bone” and it refers to any surgical operation in which a bone is cut to allow for modifications. In the present context, it is the surgery that allows the realignment of the lower limb, performed on the Femur or the Tibia. As a result of this surgery, the course of the axes and thus also the stress profile in the joints can be shifted to physiological values.

There are two basic types of osteotomy for angular deformity correction: angulation-only osteotomies, which can be opening wedge or closing wedge types, as can be seen on Figure 2.4.; and angulation with translation osteotomies, which can be straight cut or circular cut (dome). Having an osteotomy with translation means that, besides having its angle corrected, the bone is also moved (translated) in order for the deformity to be properly corrected.[4]

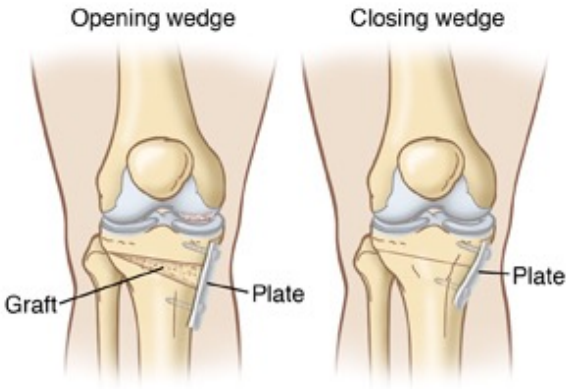

Figure 2.4. Schematics of the results of opening wedge and closing wedge osteotomy (from [D]).

The Angulation Correction Axis, known as ACA, is the axis line around which the correction is to be performed. Ideally, the ACA passes trough the CORA, resulting in what is called the ACA-CORA point, and performing the osteotomy cut trough this point results in a surgery with no undesired secondary deformities.[4] This concept can be seen on Figure 2.5.

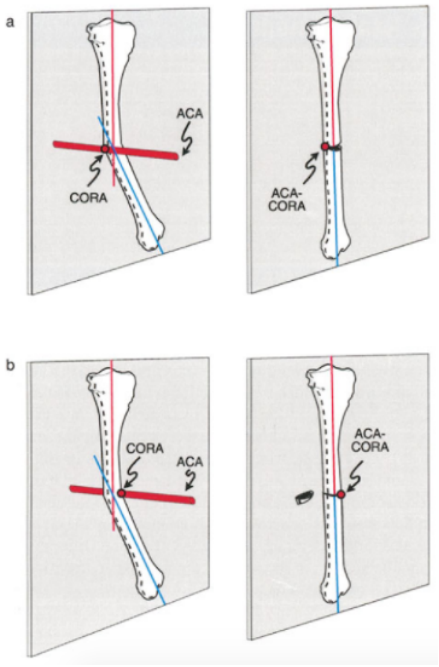

Figure 2.5. Schematics of osteotomy planning and result using the ACA-CORA concept (from [E]).

With the knowledge of the needed deformity correction and the optimal cutting point, the surgery can be performed. In a simple way, the common practice is to use the Ilizarov circular fixator to fixate the bone to be corrected, as in the example on Figure 2.6, then cut the bone as close to the ACA-CORA point as possible and then use the fixator to set the bone to the proper alignment.

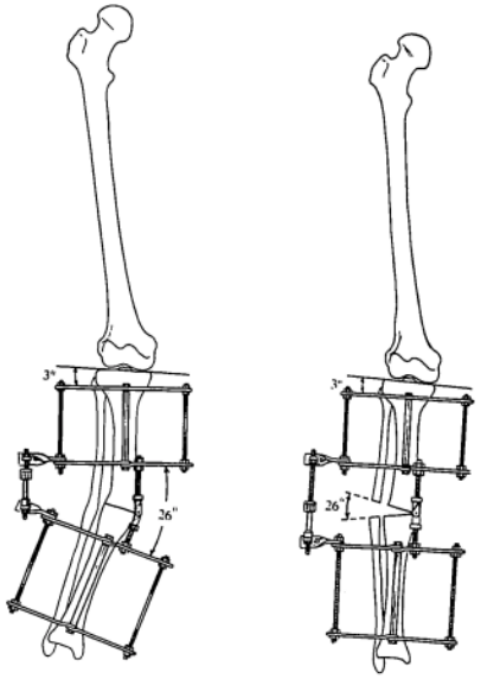

Figure 2.6. Schematics of an example osteotomy surgery using the Ilizarov circular fixator (from [F]).

In case of an external fixation osteotomy, like the one in the given example, performing the corrective osteotomy close to the ACA-CORA point is (mostly) possible and fairly easy, but in the case of a internal fixation osteotomy, there are several limitations due to the specific implant.

During the 20th century, these surgeries were performed using the “eyeball” technique, with no previous planning and a lot of improvisation from the surgeon who would just operate based on what he saw and previous experiences, which, in the 21st century, is no longer acceptable. Many innovative osteotomy techniques have been proposed over the years, with subjectively acceptable results, but objectively inaccurate, with secondary deformities resulting from primary correction. Although these secondary deformities are asymptomatic initially, they lead to degenerative changes and disability over time.[4]

Concepts like CORA are recent and allow for a better surgery planning. Nevertheless, there still is a lot of work that can be done and the planning of these types of surgery can still be improved. The further development of imaging techniques and the possibility of intraoperative navigation techniques can allow for better planning, visualization, and facilitation of the surgery.

3. STATE-OF-THE-ART

This chapter aims at exploring relevant literature concerning this dissertation's work.

3.1. CLINICALLY USED OSTEOTOMY PLANNING METHODS

Preoperative planning of osteotomy (and other deformity correction and knee surgeries) has always been necessary. When the surgery first started to be performed, this planning used to be done in a fully manual way by the surgeons, requiring the use of a ruler, scissor, goniometer and the radiograph[5]. Then, the planning evolved as templates started to be used. The surgeon would have a set of conventional templates and impose them on radiographs on the basis of best fit.

This type of planning has become less and less common as digital formats for imaging have become the standard[5] and as researchers have shown the advantages of a computer-based preoperative planning over the traditional template planning, especially when deformed anatomies are involved[6]. The accuracy and the repeatability that can be attained using this planning software is described as being the same (or better) as when planning the operation with the conventional templates.

Several software programs have been developed over the years as an alternative to the template planning, but there is little consensus on the ideal medical imaging technology that should be used[7], with CT (Computed Tomography) images being mainly used in these programs[8]. MRI (Magnetic Resonance Imaging) is not a standard in preoperative procedure, even when it has been proven that MRI scans provide the same results as CT scans for the assessment of the lower alignment[7], the first step in the preoperative planning.

A 2015 study[5] has compared 5 different well-established commercial software programs that are widely used to perform preoperative planning High Tibial Osteotomy (HTO): TraumaCad, MediCAD, Sectra, Medweb and Photoshop. Several aspects of each program were compared: the image type that can be used, the capability (or need) to use templates, the control and features offered to the user (such as automatic axis, presentation of the CORA or angle automatic calculations) and the possibility of visualizing the correction, among other things.

The study does not come to a conclusion on which software is the best, only pointing out what can be considered the strengths and weaknesses of each program. Nevertheless, one can notice that, for now, none of these popular software programs uses 3D models for the assessment of the alignment or to plan and pre-visualize results of the osteotomy.

MediCAD Knee 3D is a software developed my MediCAD that uses 3D models from patients with the purpose of supporting doctors in better planning of knee endoprosthesis. It is equipped with a measuring tool that is capable of performing what is called “traditional mesures” on the lower limb and also some other measurements that can only be performed in 3D, such as the tibial torsion and the femur torsion values, making this a clear advantage of using 3D planning software, as this type of information can not be extracted from 2D planning methods. It then allows the user to assemble the individual implant components using the implant configurator and place them into the 3D model (the patient's CT images). The implants can be adjusted, rotated, moved or changed to another implant type, in a fully interactive way, all in a 3D environment. Nonetheless, this software, as said, is only applied to the planning of knee endoprosthesis and not osteotomy, and there is no information regarding plans to adapt this software to this end.

PeekMed is a commercially available 2D/3D hybrid software system that helps orthopedic surgeons to plan their surgeries, including High Tibial Osteotomy. It is capable of automatically calculating the angle needed for the correction, while it also allows the simulation of fixation hardware implantation and the actual osteotomy. However, while the simulation can be performed using the 3D environment, no clear information can retrieved about the ability of the software to use the same 3D environment for the alignment assessment.

The fact that PeekMed was developed by a small startup company might also explain why this software is not widely known and used, and also why is also hard to find information about it. Only in August 2017 the software achieved the ISO 13485 certification, which represents the requirements for a comprehensive quality management system for the design and manufacture of medical devices, often seen as the first step in achieving compliance with European regulatory requirements, and also the CE mark, which allows PeekMed to be sold for clinical use in the European Economic Area (EEA) and Switzerland. The company is yet working on getting FDA approval in order to sell in the US market.

The fact that these more advanced softwares are still not being used to their full potential or that they are still relatively unknown in a global scale is still motivating a lot of research on novel methods worldwide.

3.2. Research on Novel Methods

3.2.1. 2D vs. 3D Methods

According to [9], measuring the lower limb alignment using two-dimensional (2D) methods can cause several issues. An improper positioning and orientation of the lower extremity while obtaining the scans often lead to ambiguous and inaccurate images, and this can’t be overcome on a two-dimensional (2D) setting. Also, deciding the best slice from hundreds of slices for marking reference axes is a hard task.

3D is specially useful to evaluate the extent of variation of lower limb alignment due to limb rotation and inclination, since these 2 factors can change the anatomic angles of the proximal Tibia in 2D imaging studies. 3D allows the rotation and inclination to be accounted for[10][11].

Researchers[12] have then concluded that 3D tools make for a better planning in comparison to 2D tools, but that the interaction with these 3D tools require some additional practice, which can be a disadvantage. The 2D tools do allow for a faster and more correct evaluation of the patient’s situation than current 3D tools, but this does not erase the pointed disadvantages.

Some papers about using 3D models for osteotomy planning may be found[9][10][12][13], but, apart from the stating that they were based on CT scans, they lack an exact description of how these models were generated. One study[11] does describe importing the DICOM data from CT scans into *Mimics* (Materialise, Leuven, Belgium) to create a 3D model of the proximal Tibia, and then, exporting it to *Geomagic* (Geomagic, Research Triangle Park, North Carolina) to get the measurements.

However, CT scanning exposes patients to a greater amount of radiation (when compared with a standard X-ray for 2D planning), and if you weigh this "cost" against the "benefits", it might not be worth it to expose the patient to this radiation in order to get a 3D model.

In that sense, a 2012 study[8] was conducted to see if measurements obtained with 3D models based on low-dose biplanar radiographs (BPR) were similar to those obtained by CT. The study found the measurements to be interchangeable, meaning that the 3D models could be obtained from a lower dose imaging system.

More recently, in 2016, researchers[14] created bone 3D models using a new acquisition protocol for BPR, the BMicroDose, that represents a combination of protocol optimization and dedicated new image processing, resulting in a much lower radiation exposure for the patient. They concluded that the osteotomy required lower limb measurements made on 3D models based on micro-dose BPR are as reliable as measurements based on low-dose BPR images, with the advantage of exposing the patients to 10-times less radiation. This study made use of the EOS X-ray machine and of the SterEOS software by EOS to reconstruct the 3D models of the lower limb.

The EOS X-ray machine is capable of performing a simultaneous capture of biplanar X-ray images by slot scanning of the whole body in an upright, physiological load-bearing position, using really low radiation doses. The images are captured in a spatially calibrated manner and allow for a precise 3D surface reconstruction of vertebrae, pelvis and other parts of the skeletal system using SterEOS.[15]

The reconstruction procedure is based on the virtual automatic manipulation of a normal human skeleton that is virtually deformed to fit the new images. The bones in the virtual 3D skeleton are shaped/deformed according to 3D coordinates of specific points on the bone surface. This procedure has been validated for various bones (vertebrae, Femur, Tibia) first using dried anatomical preparations in vitro, and then in vivo.[15]

Another study[16] has demonstrated that the alignment measurements on 3D modeling produced by the EOS system allows for a more accurate evaluation than the 2D measurements that are routinely used in clinical practice, again because the errors due to wrong limb positioning are eliminated. Once again, it is pointed out that one of the major advantages of EOS technique is that it avoids a CT scan acquisition. The main issue with SterEOS is that it is only available to owners of the EOS System, which limits its use by doctors and technicians worldwide.

There are some other commercially available 3D tools that can be used during surgery: VectorVision is an intraoperative planning and navigation system for high tibial osteotomy capable of the 3D simulation of the expected osteotomy result[12]; navigation systems provided by TraumaCad and MediCad can provide real-time information, which is revolutionary for orthopedic surgeons who

correct alignment during surgery[11]. These systems are an example of the trust on software that uses 3D simulation.

But with the high cost compared to the number of patients per year, most hospitals in development countries cannot afford to buy these highly advanced software programs[5], which can be considered not necessary as of now on a software for osteotomy.

One can then come to the conclusion that using 3D models for the assessment of the lower limb alignment and for osteotomy planning is an advantage, and, as stated before, there have been some software programs developed. The main problem with these is that they are still too expensive and maybe difficult to use, so development of cheaper easy-to-use new software has a lot of potential.

3.2.2. Experimental 3D Software for Alignment Assessment

The 3D method described on [10] can be used for the assessment of lower limb alignment. It uses thin-slice CT images to recreate a 3D model and relies on geometrical manipulation of the model to find a limited number of angles and axis. It was developed to study the effect of rotation on the assessment of the lower limb alignment and actual clinical usage for the assessment is not discussed.

This method uses models of the Femur, Tibia, and patella, created using Analyze PC 3.0, a surface rendering software. The program requires four landmark points to be plotted on the 3D surface models: the first point is the center of the femoral head, obtained by finding the center of the best-fit sphere; the second and third points are the top of the medial and lateral femoral epicondyles; and the fourth point is the centroid of a series of points on the distal tibial joint surface that were surrounded by a manually drawn circle. They are used for anatomic reference and also to access orientation.

The software then projects the 3D model on the 2D XZ-plane and calculates the Femur Torsion Angle (FTA) and the Hip-Knee-Ankle angle (HKA) as indices of lower limb alignment, where FTA is the lateral angle at the intersection between the femoral shaft axis and the tibial shaft axis, and HKA is the medial angle deviation from 180º at the intersection between the mechanical axes of the Femur and Tibia. Additional points need to be found in order to access all the axes. They are manually identified by creating cross-sections on the bones and finding the centroids of these sections.

The software described on [9] was developed using the C++ language and it uses 3D bone models reconstructed from CT scan images to fully automatically extract six specific anatomical landmarks on the lower limb. The program integrates volumetric data and triangular meshes of bone models together to recognize the anatomical landmarks. While the triangulated surface model data is necessary for geometric landmark localization and rapid rendering, the volumetric data is important for axis computation.

The first landmark is the center of the Femur head and it is found by automatic recognition of Femur head mesh by a volume-based shape function and then, using four points on its surface, a sphere is created and the point corresponds to its center. The femoral anatomical axis, the Femur neck axis and the Tibia anatomical axis, are three landmarks found by an algorithm that generates the mid-diaphyseal (medial) curve of the bones and then finds points on this curve that allow for the generation of the landmarks. The Femur condyle axis is found by automatically finding the medial and lateral most distal points of the Femur and connecting these to the femoral condyle center (which is obtained by the intersection of the femoral anatomical axis with the model surface), resulting in a single point.

The last landmark, the Tibia plateau axis, is found my calculating the lowest points on the two concave of the Tibia pleateu and connecting them.

With the landmarks found, the software then calculates the FTA and the Tibia Torsion Angle (TTA), that are then used for the assessment of the alignment.

Another group of researchers[13] developed computer-aided methods for automatically measuring anatomical deformities on the lower limb using 3D bone models reconstructed from CT scan data.

The overall procedure of this method goes as follows: first, the 3D models of the lower limb are reconstructed from CT scan images; then, the required anatomical landmarks are identified; the third step is to compute the medial axis of long bones; this then allows for the reference axes to be computed from anatomical landmarks and medial axes; after this, the reference centres from anatomical landmarks are identified; the sixth step is to measure the torsional deformation using the reference axes; then, the angular deformation angles can be measured using the anatomical and mechanical axes; and finally, the long bone curvature deformation can be calculated in the medial axis.

The landmarks on the Femur and Tibia bone models are said to be automatically identified based on their intrinsic geometric characteristics, using geometric algorithms, specifically curvature derivatives, one for each landmark. The landmarks are then identified and labelled based on their unique spatial-adjacency configuration with other landmarks. These methods were developed using C# language .

None of the above described software programs is known to have become commercially available.

The advantage of a fully automatic approach is the elimination of the variability and human induced errors in measurements in manual methods. But such approach might increase the time needed for the evaluation of a patient to a point it could surpass the time needed for an experienced surgeon to do a manual “standard” evaluation.

4. PROJECT OVERVIEW

After an introduction to the topic of lower limb deformities and osteotomy planning, and the state-of-the-art on methods for such planning, the dissertation's motives and goals are defined in this chapter.

4.1. MOTIVATION

This project results from a cooperation between the research group CAPS - Computer Aided Plastic Surgery - from the *Klinikum Rechts der Isar* of the Technical University of Munich (TUM), and the *3D Chirurgie* group from the *Klinik für Allgemeine, Unfall- und Wiederherstellungschirurgie* of the Ludwig-Maximillian University (LMU), also located in Munich.

The two groups plan to develop a method for the preoperative planning of deformity correction and knee surgery to be used in clinical context by the *3D Chirurgie* group, which is responsible for the planning of osteotomies on a regular basis, but still uses a manual method for the alignment assessment. The LMU group wishes to make use of new available technology and modernize its planning methods. For this, 3D models of patients' bones using CT/MRI data should be generated and, ultimately, a semi-automated workflow for planning the needed osteotomy surgery should be developed and validated.

Following these plans, a project consisting of developing a new software for assessing the lower limb alignment based on 3D models was proposed and carried out during a 7-months internship, resulting in the work on which this dissertation is ultimately based on.

4.2. OBJECTIVES

For the completion of this project, a number of objectives was set in order to allow for a more logical and sequential workflow and also to ensure the best outcome possible. Each objective can be considered as a stage of the project. The objectives, in the order they were to be achieved, were the following:

- To generate best possible quality 3D models of different patient's lower limbs, using both segmentation and 3D rendering software. Also, to ensure that these models can be generated by any user and that this will not cause a source of massive variability/error in the final outcome;

- To understand the exact angles and measures desired by the *3D Chirurgie* group and the therefore needed anatomic landmarks for the alignment assessment;

- To design a program that uses the generated 3D models and, in the most automatic way possible and with an easy-to-use interface, returns all the needed angles and measures.

- To ensure that the program is reliable and consistent in its results in both intraobserver and interobserver domain and that it can replicate the manual assessment by comparing the results obtained by using the program with manual assessment results.

5. 3D MODELING OF THE LOWER LIMB

The first step for the 3D alignment assessment is to create the 3D anatomical model of the patient. Several models were reconstructed from anonymized 2D CT scans provided by the *3D Chirurgie* group using the *Mimics 14.0* software. This software was used due to its availability, to the fact that it had been used before by other members of the research group, and also because previous research[11] had also used it.

For the development of the alignment assessment software, the goal was to have models that were relatively different from each other regarding their quality (models based on different quality CTs) and their anatomical contents (models made from female and male patients, with different types of deformities). Having different models to use to develop the software would guarantee that it could be used on different scenarios.

The following sections of this chapter explore how the 3D models were obtained and prepared to be used by the developed software. A specific example from a patient, from now on Patient 1, is followed throughout the chapter. Patient 1 is deceased, so it was possible to obtain a very high resolution CT (1691 slices with a layer thickness of 0.62 mm), since radiation exposure didn't need to be considered. Due to the expected high accuracy of the resulting 3D model, this case was to be used for the development of the software after successful segmentation.

5.1. SEGMENTATION

As previously stated, the *Mimics 14.0* software was used to create the models, more specifically, to segment the CT images and then calculate the 3D models. The software displays the data in all three anatomical views (transverse, sagittal and coronal) simultaneously and, by moving the mouse wheel with the cursor over one of the views, the user can scroll through all the different slices. It also allows the user to work on a specific view on full screen mode, which eases certain tasks.

After the previously anonymized CT images were imported into *Mimics*, a threshold segmentation was performed using the dedicated tool. The "Bone (CT)" presetting, which limits the HU values to the interval 226 - 3071, was used. This allowed to automatically separate all bony structures, as can be seen in Figure 5.1.

It was decided that creating a separate mask for each section/bone (i.e., the Femur, the patella, and the Tibia and fibula together) would be useful further on. For this, the "Region Growing" function was used to select contiguous sections on different slices and create one unique separate section. However, all other connections that should not be part of the model but were created by using this tool,

had to be removed manually. To this end, the “Edit Mask” function was used, by which the user can delete incorrectly marked areas or select/mark desired areas, adding to the mask.

Since only the surface of the bone is relevant to the alignment assessment, structures like the hole inside the Femur shaft don't need to be considered, and therefore were ignored to simplify the model generation.

After the segmentation was complete, various default settings for the “3D Calculation” tool were available - Low, Medium, High and Optimal - which differ in the fineness of the resulting model. The “Optimal” setting is the one recommended by the program, so it was used.

In Figure 5.2, three fully segmented CT slices can be seen, one per anatomical view. The different masks created are represented in different colors. On the lower right square, the calculated 3D models can be seen. These models were then exported under the STL format.

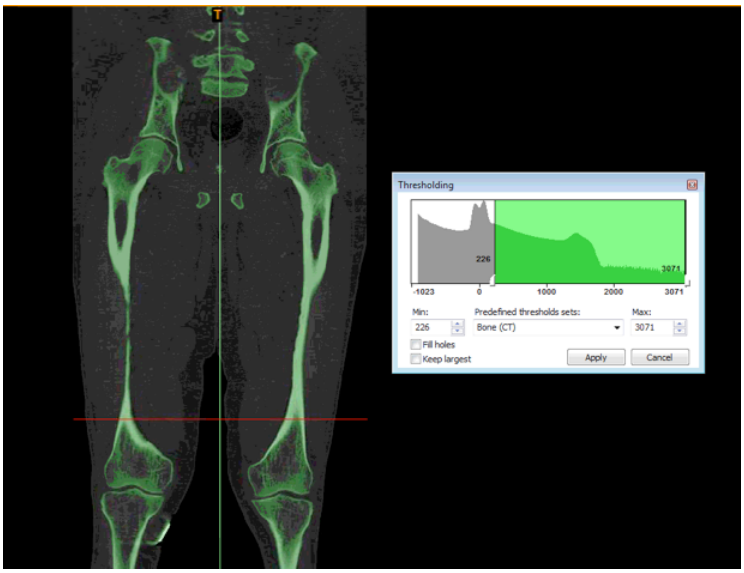

Figure 5.1. Threshold segmentation result on Patient 1 using the dedicated tool and “Bone (CT)” setting in *Mimics*.

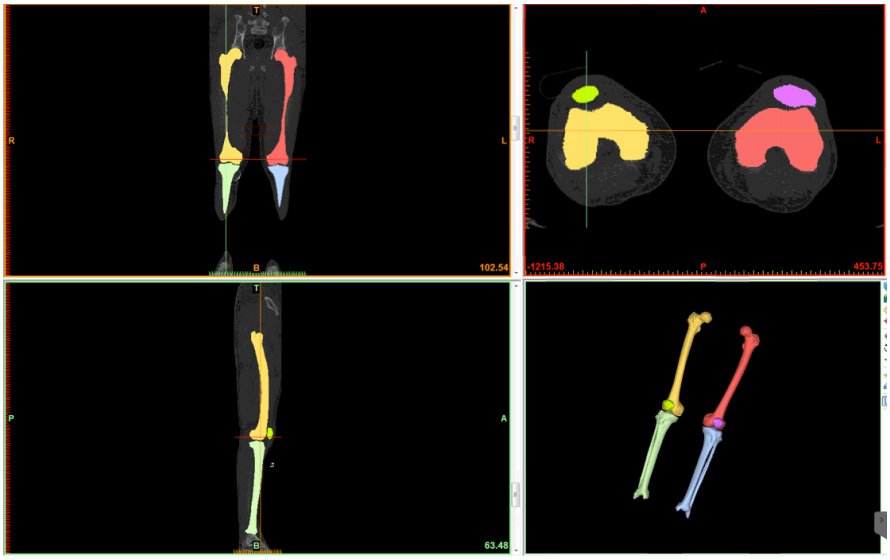

Figure 5.2. Completed segmentation of Patient 1 and resulting 3D models in *Mimics*.

5.2. Optimization and Preparation

After the segmentation step, 3D models are obtained, but they are still not ready to be used: their quality needs to be confirmed and optimized if needed, and they need to be set up in a certain way in order to be efficiently used by the software, so that computation time is minimized and so that the accuracy is the best possible. For this end, the *Geomagic Studio 14* software was used, again due to the program availability, to the fact that it had been used before by other members of the research group, and also because previous research[11] had also used it.

After loading the generated models into *Geomagic,* the first step on this optimization and preparation process was to check the mesh quality and remesh the model if needed. The finer the mesh, i.e., the smaller the triangles that constitute the model are, the better quality it has. In this sense, it was decided that the maximum edge length accepted would be 1 mm. As a consequence, any model that presented an edge length larger than this value was remeshed using the dedicated tool, preserving all edges and boundaries. An example of remeshing can be seen in Figure 5.3.

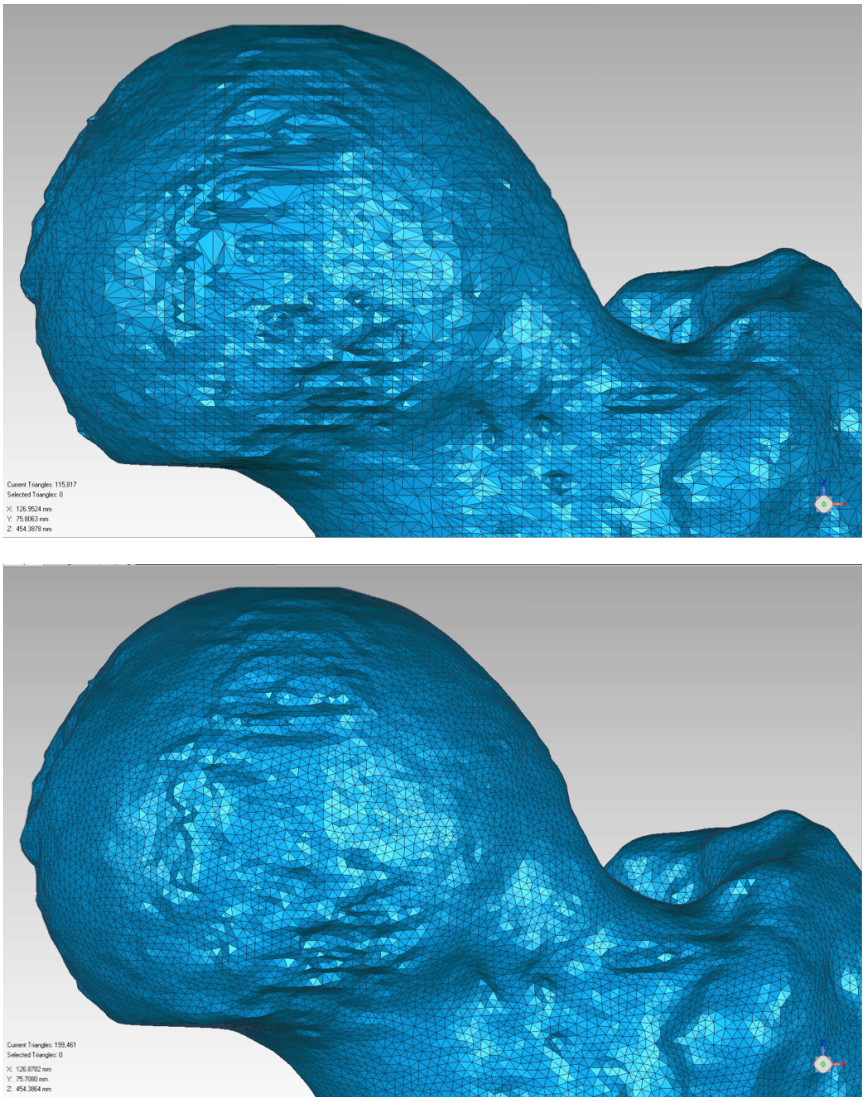

Figure 5.3. The mesh over the Femur head before (Above) and after (Below) remeshing. The number of elements was raised from 115 817 to 199 461, with the triangle edge length changing from 1.256 mm to 0.905 mm on the Femur model. The mesh is visible finer and details on the bone are more visible.

In present-day clinical context, the alignment assessment is based on conventional long standing leg X-ray acquisitions, in which the patella is aligned in a way so that it lies centrally between the femoral epicondyles, with its anterior face facing forwards. For this reason, it was decided that the alignment of the models within the coordinate system has to correspond to the alignment of the leg in this acquisition method.

Furthermore, since the assessment process is based on anatomical landmarks that can be/are found trough methods that are geometry-dependent, a proper orientation of the models is crucial. For example, if one wants to find the most anterior point on a model, which would correspond to the maximal/minimal value on a certain world-axis, having the anterior surface of the bone correctly positioned in relation to this axis is needed (in this case, the most perpendicular possible), or the wrong point would be found.

Thus, the patella model was rotated using the "Object Mover" tool so that its anterior face would be correctly positioned, as can be seen in Figure 5.4 and a rotation matrix was automatically created by *Geomagic*. This matrix was then used to rotate the other bones/models using the "Transform" tool.

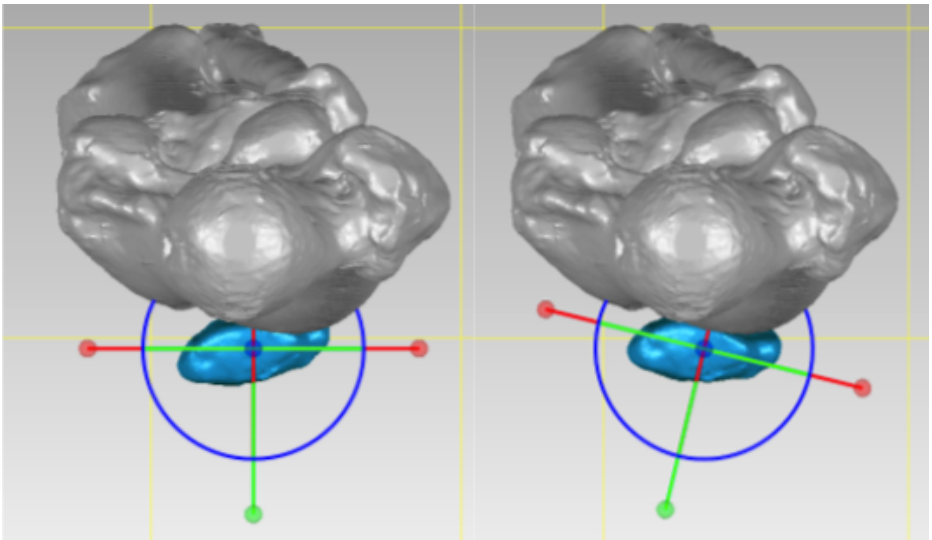

Figure 5.4. Patella model before (Left) and after (Right) reorientation.

With the models properly aligned, the final step of the preparation step could take place. In order to standardize the process, the bones must be named in a certain specific way. Also, it was decided that it is best to separate the proximal and distal portions of the bones, creating two separate models, so that the program has less triangles to go trough to find each point. An example of this separation procedure using the "Trim" tool can be seen in Figure 5.5.

It was decided that the following naming order would be used: firstly, the leg side must be identified, i.e., "Left" or "Right"; secondly, the specific bone is identified, the options being "Femur" and "Tibia"; and finally, the portion of the bone is identified, which can be "Proximal" or "Distal". It is not important to properly name the patella as it will not be used by the program and it's also not relevant to separate the Tibia from the fibula, so the name of the first is used to describe the two. In this way, the proximal part of the left Femur bone must be named "Left Femur Proximal".

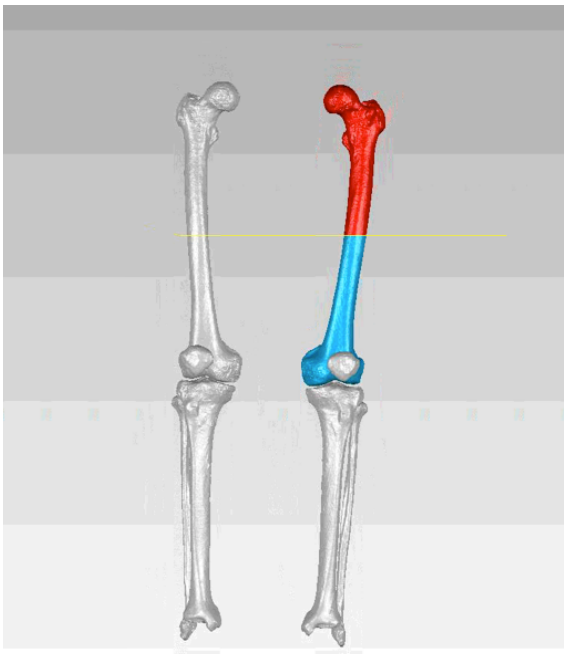

Figure 5.5. Example of bone (here, the left Femur) separation into the proximal (in red) and the distal (in blue) sections.

5.3. User Influence on Model Generation

The program is being/was developed to be used in a real-life context. This means that, unless someone is made responsible to create every single 3D model, which is unlikely, different users will have to create different models. Therefore, testing the influence of different users on the model generation is necessary.

Three different users created their version of a 3D model of Patient 1 following the steps previously described. All users had previously worked with *Mimics*, but User 1 has virtually no experience segmenting medical images, User 2 has some experience, and User 3 is very used to segment this type of images, particularly with the used software.

For comparison, it is best to evaluate the models of the individual bones and not the whole model of the lower limb. Consequently, in Table 5.1 the volume of the different models generated by the three different users can be analyzed. The average volume was calculated from the three users and the percentual individual difference from each user to this average was calculated.

One can observe that every model has a difference of less than 1% from the average value, which means they are very similar. The same conclusion can be drawn from the more usual statistical concepts calculated: the standard deviation and the mean absolute deviation (M.A.D.), which gives the average distance between each data point and the mean. Both of them take very small values for every model, indicating that they are indeed very similar to each other.

In Table 5.2 the number of elements on each model can also be compared. From the values of the standard deviation and specially the M.A.D., once again, one can come to the conclusion that the models are very similar.

This means that different users, even with different backgrounds of expertise, will create very similar models to be further used for the alignment assessment. It can not be said that the user influence is non existent, but the models generated were similar to the point the results won't probably be very affected by these small differences.

Table 5.1. Comparison of the generated model's volume.

	Mean (cm^3)	User 1 (cm^3)	% Diff. from Mean - User 1	User 2 (cm^3)	% Diff. from Mean - User 2	User 3 (cm^3)	% Diff. from Mean - User 3	St. Deviation	M.A.D.
Left Femur	4,371.898	4,364.697	0.165	4,371.434	0.011	4,379.563	0.175	7.444	5.110
Left Patella	54.255	54.253	0.004	54.257	0.003	54.256	0.001	0.002	0.002
Left Tibia + Fibula	3,472.971	3,444.943	0.807	3,485.264	0.354	3,488.706	0.453	24.334	18.685
Right Femur	3,609.250	3,605.911	0.093	3,605.704	0.098	3,616.135	0.191	5.963	4.590
Right Patella	53.320	53.282	0.071	53.212	0.203	53.466	0.274	0.131	0.097
Right Tibia + Fibula	3,395.724	3,391.993	0.110	3,394.448	0.038	3,400.732	0.147	4.507	3.338

Table 5.2. Comparison of the generated model's element number after remeshing.

	User 1	User 2	User 3	Mean	St. Deviation	M.A.D.
Left Femur	199,461	198,880	198,740	199,027	382	289
Left Patella	12,994	13,082	12,950	13,009	67	49
Left Tibia + Fibula	195,791	196,194	195,702	195,896	262	199
Right Femur	201,298	200,662	200,468	200,809	434	326
Right Patella	13,046	13,030	13,116	13,064	46	35
Right Tibia + Fibula	195,984	195,768	195,718	195,823	141	107

6. PROGRAM CONCEPTION & DESIGN

The core of the project was the design of a computer program/software that could do the alignment assessment of the lower limb in the most automatic way possible. In the next chapters, the conception and development of this software is described.

The specific landmarks and the angles that the program should/must find are firstly identified and then the process by which they are properly found and/or calculated is described. Lastly, the finished program, with its user interface, is presented.

6.1. DEFINITION OF DESIRED ANGLES AND MEASURES

For a proper alignment assessment, specific angles must be found. Some of these angles are standard in the assessment procedure, but some angles which provide some additional information may or may not be deemed necessary by some specialists. The angles and measures that should be found by the developed program were decided by specialists of the *3D Chirurgi*e group, based on their clinical knowledge and sense of need for a better planning. Successfully finding these angles is to be the primary function of the program.

As previously stated, there are two axis that are very important in the alignment assessment: the mechanical axis and the anatomical axis of the leg.

The leg mechanical axis goes from the hip joint (or the center of the Femur head), through the knee joint and down to the center of the ankle. One can also evaluate the two bones involved in this axis separately, resulting in a femoral mechanical axis and a tibial mechanical axis. The angle between these two axes is called the Hip-Knee-Ankle angle, usually identified as HKA, and it should have a value close to 180º, both in a frontal or sagittal anatomical plane view.[17]

Also, as previously seen, the distance measured between the mechanical axis of the lower limb and the center of the knee joint is known as the Mechanical Axis Deviation, or MAD. This deviation can be observed in both horizontal and vertical axes (or X and Y axes) from a transversal anatomical plane perspective.[2]

A bone torsion angle is the angle between an axis that crosses one end of a bone and an axis that crosses the other end, caused by a twist about its longitudinal axis. It can be measured in both Femur and Tibia.

For the femoral torsion angle, two lines are needed: the Femur neck axis, that goes trough the center of the Femur head and the center of the Femur neck, and the most distal transcondylar line, i.e. a line tangent to the posterior points of the femoral condyles.[18] According to [19], the expected

normal value of this angle is 24.1 ± 17.4°. The angle formed between the line tangent to the posterior points of the femoral condyles and the world's x-axis was considered of interest to the assessment and for that reason it was also evaluated under then name of "Position of the Condyles".

The Tibia torsion angle, which has an expected normal value of 34.9 ± 15.9°[19], corresponds to the angle formed by the line tangent to the tibial condyles and the distal reference line, which is formed by intersecting the centers of the medial and the lateral malleoli[20]. The angle formed between this distal reference line and the world's x-axis was deemed relevant to the assessment and, therefore, it was also recorded under the name of "Position of the Malleoli".

Besides these more generic and more easily determined angles and measures, there is further anatomical and mechanical information specified in [4] that can be extracted from the lower limb, as can be seen in Figure 6.1.

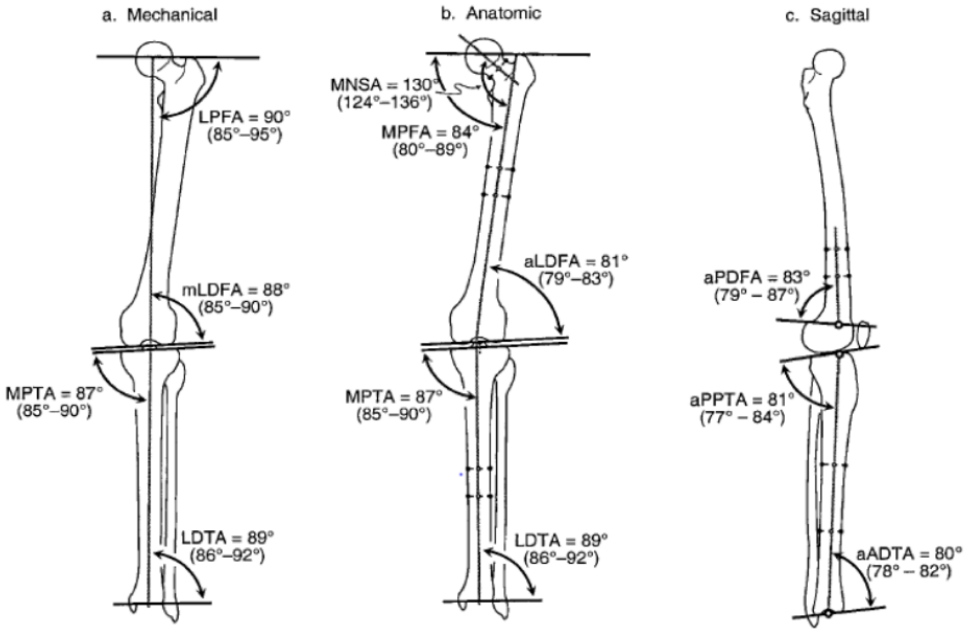

Figure 6.1. Further angles for alignment assessment defined by D. Paley (from [E]).

Starting with the mechanical angles, the Lateral Proximal Femoral Angle, usually identified as mLPFA, or simply LPFA, is formed by the line that goes from the center of the femoral head to the top of the greater trochanter, and the leg mechanical axis, which results in an angle of about about 90.0 ± 5.0° at normal anatomical axis ratios.

The mechanical Lateral Distal Femoral Angle, known as mLDFA, indicates the position of the femoral knee joint surface with respect to the femoral mechanical axis in the frontal plane. For the determination of this angle, a tangent to the most distal points of the Femur condyles is defined and then the angle to the mechanical femoral axis is determined, which should be approximately 87.5 ± 2.5°.

Another mechanical angle, the Medial Proximal Tibia Angle, or the MPTA, as it is known, is formed by the line of the proximal tibial surface is defined by the two outermost points (medial and

lateral) of the tibial plateau, and the tibial mechanical axis. The normal value of the MPTA is approximately 87.5 ± 2.5° as for the mLDFA, however, the MPTA should always be slightly smaller than the mLDFA.

Proceeding to the anatomical angles, the Medial Proximal Femoral Angle, known as aMPFA or simply MPFA, is the angle formed between the line connecting the center of the femoral head to the top of the greater trochanter and the femoral anatomical axis. The expected value for this angle is of about 83.0 ± 5.0°.

The angle of the Femur neck is given by the Centrum-Collum-Diaphysis Angle, known as CCD, defined as the angle between the previously defined Femur neck axis and the femoral anatomical axis, and, at normal anatomical axis ratios, presents a value of 130 ± 5.0°.

The tibial slope indicates the inclination of the tibial plateau in the sagittal plane and it is evaluated in terms of the Posterior Proximal Tibial Angle, or PPTA as it is known. This angle is defined by the position of the tangent line to the proximal Tibial proximal surface with respect to the anatomical axis of the Tibia. Since the tibial proximal surface is formed by two condyles, it makes sense to differentiate between a medial and a lateral tibial slope, and deformities tend to affect one side more than the other. The expected value for both slopes is 80.5 ± 3.5°.

Table 6.1 contains a summary of every angle and measure deemed necessary and the respective normally expected values, when applicable.

Table 6.1. Necessary angles and measures and respective normal values

Angles and Measures	Acronym/Representative Name	Normal Value
Hip-Knee-Ankle Angle	HKA	180º
Mechanical Axis Deviation	MAD	0
Femur Torsion Angle	FTA	24.1 ± 17.4°
Position of the Condyles	-	-
Tibia Torsion Angle	TTA	34.9 ± 15.9 °
Position of the Malleoli	-	-
Lateral Proximal Femoral Angle	LPFA	90.0 ± 5.0°
(Mechanical) Lateral Distal Femoral Angle	mLDFA	87.5 ± 2.5 °
Medial Proximal Tibia Angle	MPTA	87.5 ± 2.5 °
Medial Proximal Femoral Angle	MPFA	83.0 ± 5.0°
Centrum-Collum-Diaphysis Angle	CCD	130 ± 5.0°
Medial Posterior Proximal Tibial Angle	Medial Tibial Slope/Medial PPTA	80.5 ± 3.5°
Lateral Posterior Proximal Tibial Angle	Lateral Tibial Slope/Lateral PPTA	80.5 ± 3.5°

6.2. Definition of Desired Landmarks

In order for all the defined axes and angles to be computed, very specific landmarks on the lower limb need to be found. The exact position of where these landmarks should be were also decided by specialists of the *3D Chirurgi*e group, based on their clinical knowledge.

The points deemed necessary are presented below by section of the bone, in a proximal to distal, lateral to medial and anterior to posterior order. The exact way they are to be found is further explored later on this work.

6.2.1. Landmarks on the Femur

In the proximal end of the Femur, the landmarks to be found are: the center of the hip joint, which corresponds to the center of Femur head, the top of the greater trochanter and the center of the Femur neck. The location of these points on a Femur 3D model can be seen in Figure 6.2. The top of the greater trochanter is logically to be evaluated on the frontal view.

In the other end of the Femur, the landmarks to be found are: the most posterior points of the lateral and medial condyles, the center of the intercondylar fossa/notch and the most distal lateral and medial points. These points are represented on a Femur 3D model in Figure 6.3. The most posterior points of the lateral and medial condyles are evaluated on the transverse view.

The Femur shaft does not possess any relevant anatomic landmarks, but since some measurements require a line that goes trough the shaft, the definition of two points, a proximal point and distal point, in the center of the shaft was deemed necessary. It was decided that these points should lie approximately at one-third and two-thirds of the total length of the shaft. A representation of these two points on a Femur 3D model can be seen in Figure 6.4.

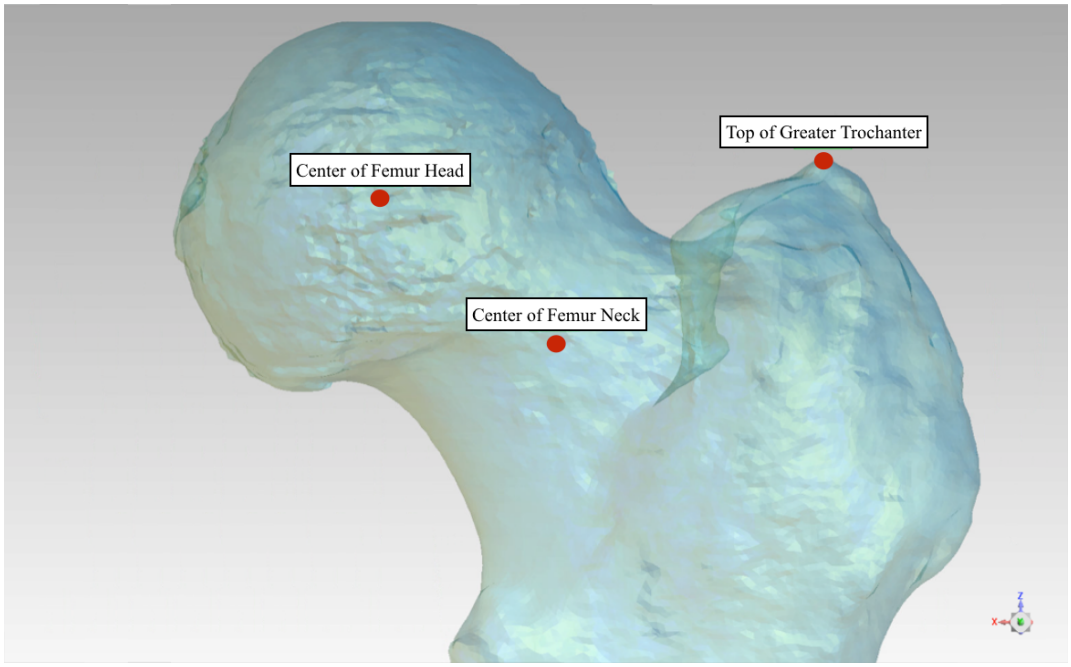

Figure 6.2. Landmarks on the proximal end of the Femur.

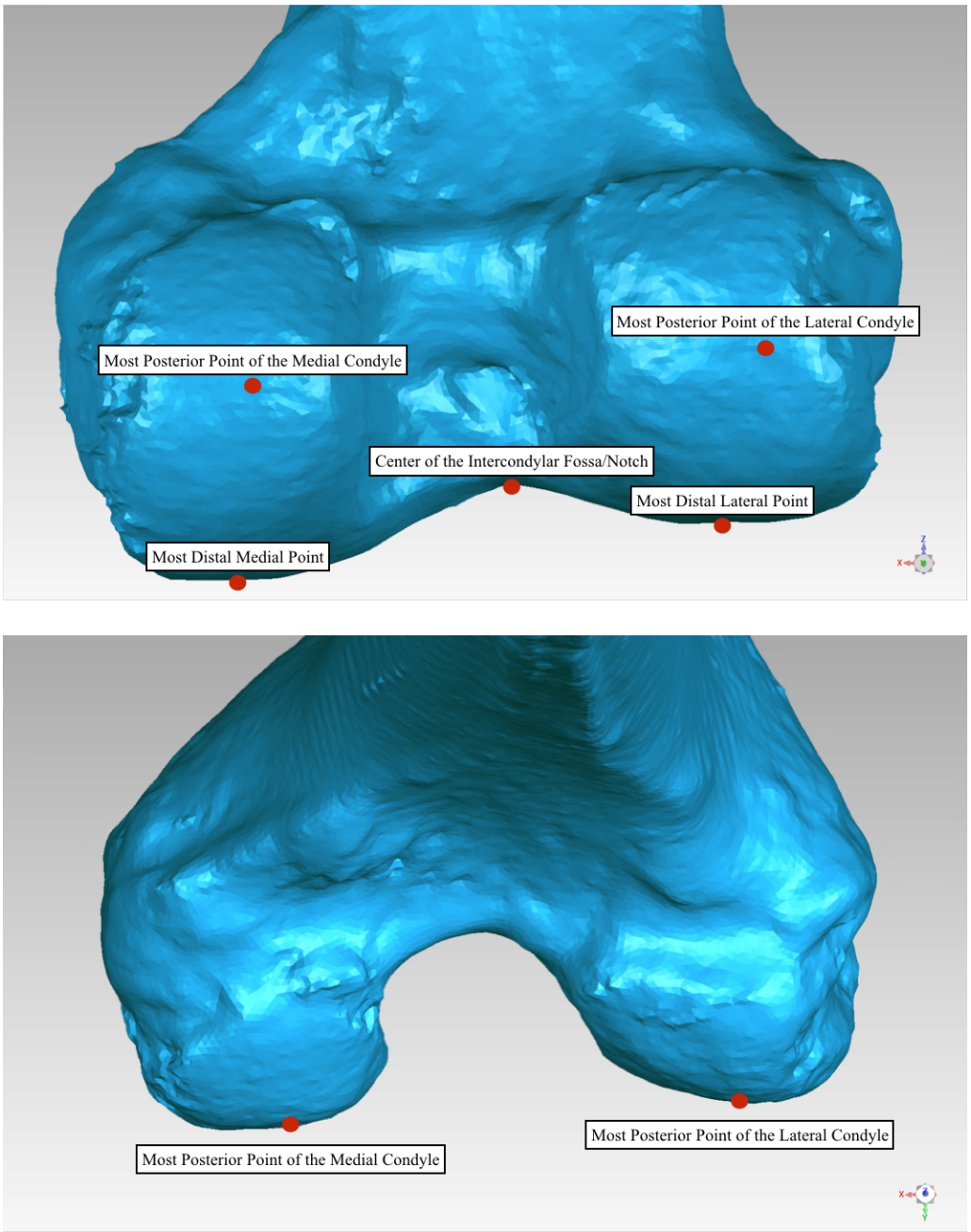

Figure 6.3. Landmarks on the distal end of the Femur.

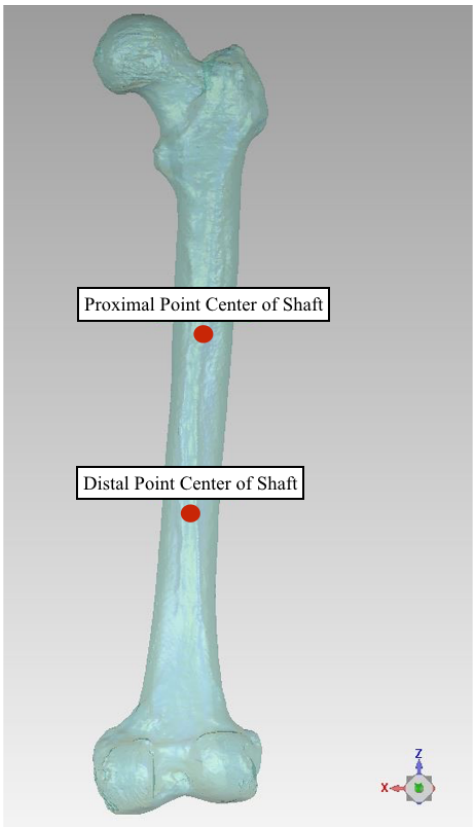

Figure 6.4. Landmarks on the shaft of the Femur.

6.2.2. LANDMARKS ON THE TIBIA

In the proximal end of the Tibia, the landmarks to be found are: the lateral and medial intercondylar tubercles, the center of the knee joint, the most anterior points of the lateral and medial condyles, the most proximal and lateral point of the Tibia plateau, the most proximal and medial point of the Tibia plateau and finally the most posterior points of the lateral and medial condyles. The location of these points on a Tibia 3D model can be seen in Figure 6.5. The points located on the intercondylar tubercles are to be evaluated on a frontal view, while the other points are to be found on a transverse view, with the exception of the the most proximal and lateral point and the most proximal and medial point of the Tibia plateau, which are to be evaluated on both anatomic views.

In the other end of the Tibia, the landmarks to be found are: the most medial point of the medial malleolus, the most lateral point of the lateral malleolus and the center of the of the inferior articular surface of the Tibia/middle point of the tibia bearing area. These points are represented on a Tibia 3D model in Figure 6.6.

As with the Femur shaft, the Tibia shaft does not present any relevant anatomic landmarks, so, once again, two points, a proximal point and distal point in the center of the shaft were defined, also lying approximately at one-third and two-thirds of the total length of the shaft. A representation of these two points on a Tibia 3D model can be seen in Figure 6.7.

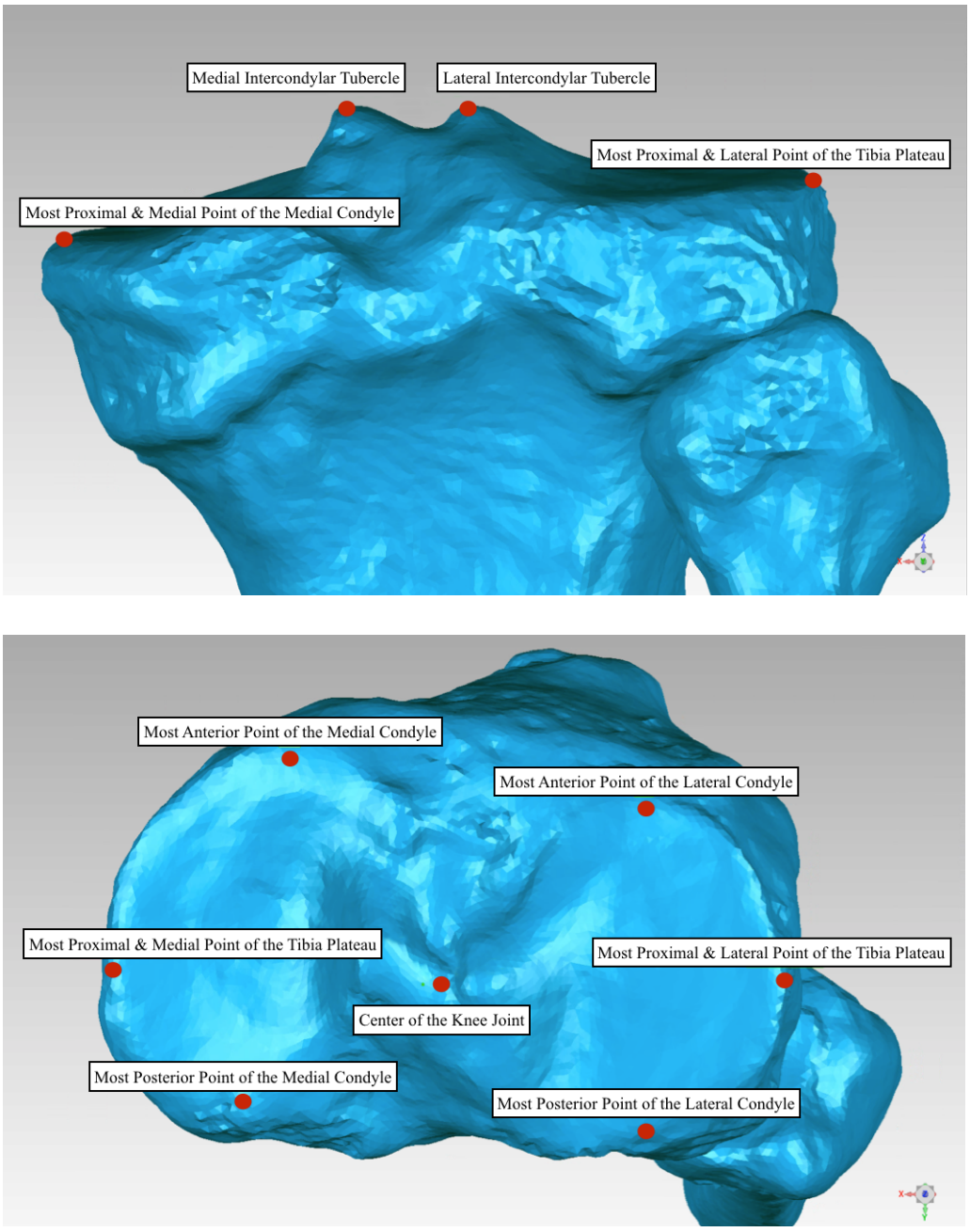

Figure 6.5. Landmarks on the proximal end of the Tibia.

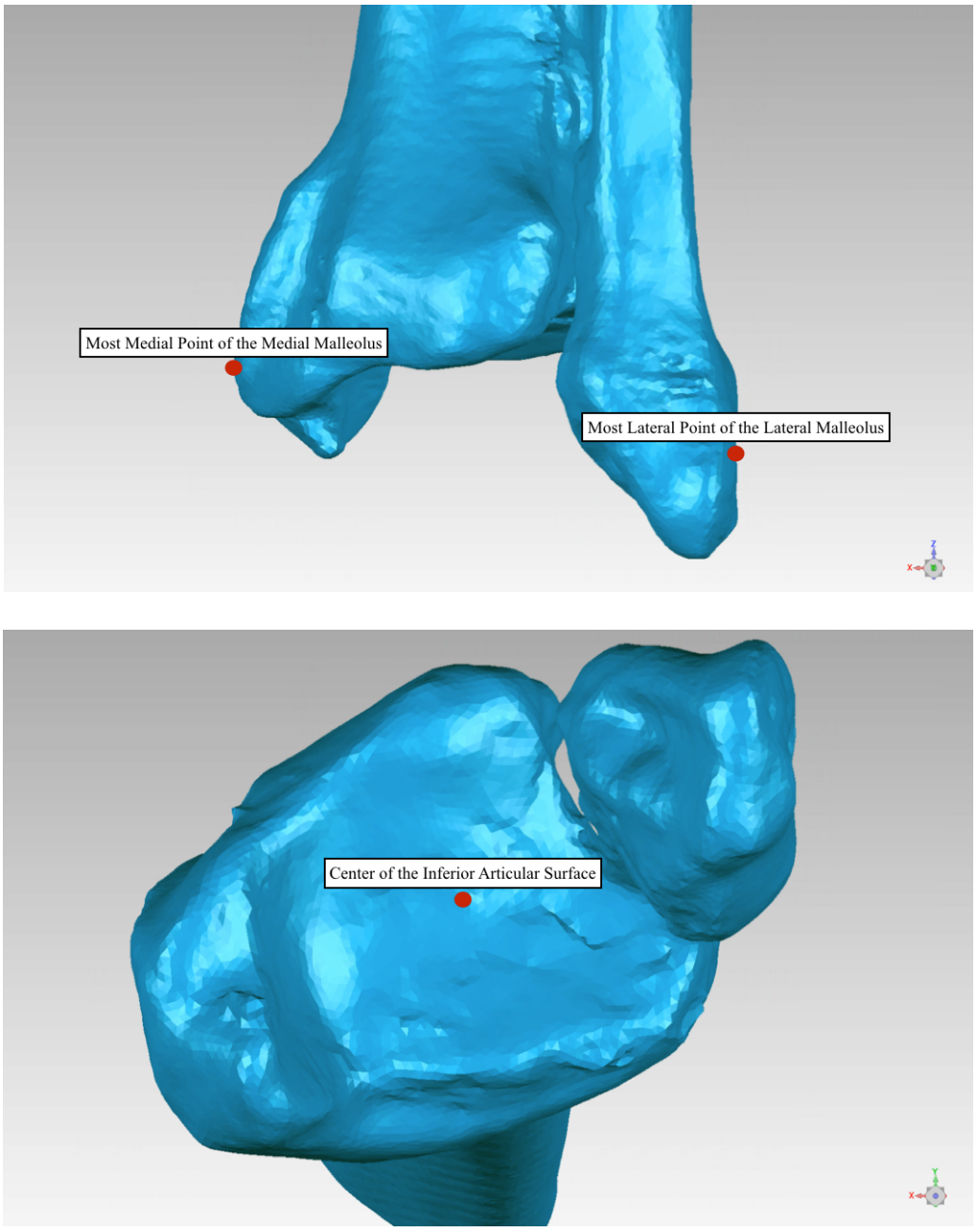

Figure 6.6. Landmarks on the distal end of the Tibia.

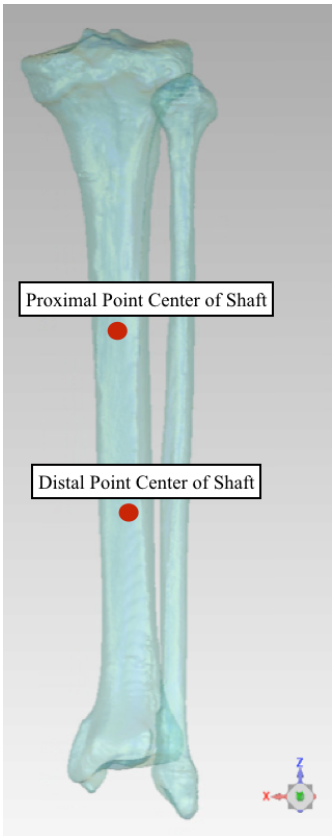

Figure 6.7. Landmarks on the shaft of the Tibia

6.3. SCRIPT DEVELOPMENT

Geomagic Studio 14 accepts user-created scripts to run on a built in scripting engine, so that those who wish to automatize their workflow can create *macros* (scripts) that use the Python programming language. Therefore, the program was developed using this programming language, specifically Python 2.7. However, *Geomagic* provides its users with an extension to the standard Python language in the form of modules - *geomagic.api* and *geomagic.app* - that can work directly on the app in a functional way, therefore facilitating the development of *macros*.

The dedicated scripting feature of the software allows the creation of additional calculations that are not part of the standard *Geomagic* offerings; the addition of *Dialogs*, the name used for user interfaces; and also the automatization of operations.

Some previous scripts developed by the CAPS group allowed finding some anatomic landmarks on 3D models using *Geomagic* but these not only required the user to have some knowledge about how to work with the software and how to retrieve information from it, but also of how to edit scripts so they would work on each specific patient, which limits its users to those with programming skills. Also, only very specific points could be retrieved using these scripts.

So, in the first place, it was decided that the user should be able to do everything from inside the program, with no programming needed, and that it should require the least amount of knowledge

on how to operate *Geomagic*, so every task should be simple and straight-forward. This influenced not only the user interface, which will be explored in a later section, but also the landmark finding itself.

The points in the center of Femur head and the center of the Femur neck should lie in the center of clearly distinguishable anatomic areas - the Femur head and the Femur neck - so the task of finding them can be treated as finding the centroid, i.e. the mean position of all the points in all of the coordinate directions of the respective geometrical volume.

One of the first problems to be detected was that, sometimes, getting a good quality segmentation of the Femur head was not possible, which would result in incorrect results if these poor-quality heads (sometimes even incomplete) were treated as the volume from which to get the centroid. In that sense, it was decided that a sphere that would fit the Femur head in the best way possible should be automatically created and that the center of this sphere would correspond to the desired point.

To maintain a standard, this sphere is to be created in both good-quality and poor-quality models. Instead, it was decided that the user can create this sphere by using the whole head as a base, which is possible when the model is complete, or by selecting 4 points distributed across the head and create the sphere from them, which is a best suit for incomplete models. The *Geomagic* extensions for Python were used in both cases to create the sphere automatically, in the first case by using the *BestFitSphere* class and the *FitSphereFrom4Points* class in the second case. Having the sphere created, its center was retrieved and labeled as the center of the Femur Head.

The functions under the class *Selector* are used to retrieve selections made on the mesh of the 3D model, on which some classes like *BestFitSphere* work upon.

Since no standard three-dimensional geometry can be fitted to the neck shape, it was necessary to set up an algorithm that could calculate the centroid that would then be labeled as the center of the Femur neck. The relevant area has to be selected and the *getActiveTriangleSelection* class receives this selection and considers it the Femur neck.

For this, it was first necessary to turn the model's triangular mesh into individual points that could be iterated. The *CreatePointsFromMesh* class was used for this end. Having created the points, Equation 6.1 was used as a guide for code implementation in order to get the coordinates of the centroid. The sum of the coordinates of every point in the selection, divided by the total number of points, results in the centroid.

$$Centroid(x,y,z) = \left(\left(\frac{\sum point\ x\ coordinates}{Total\ number\ of\ points}\right),\left(\frac{\sum point\ y\ coordinates}{Total\ number\ of\ points}\right),\left(\frac{\sum point\ z\ coordinates}{Total\ number\ of\ points}\right)\right) \tag{6.1}$$

This process of finding the centroid was reused to find several other points, with the needed adaptations. In the case of the center of intercondylar fossa notch and of the center of the inferior articular surface, both located on concave surfaces, the centroid calculation results in a point that, while it lies in the exact x and y mean coordinates, due to the inward curving, ends up being located in an unwanted z coordinate outside the surface of the model. In these cases, the way the program finds the points had to be changed so that the point would be placed on the surface of the model.

The solution found for this problem was creating a vector that is parallel to world's z-axis and that passes trough the point found by the algorithm, so that it intersects the model's surface, and then retrieving the intersection point by using the *IntersectMeshWithRay* class.

The points located along the femur's and the tibia's shaft were also calculated using the centroid method, but with specific adaptations. Since these two points are to be located approximately at one-third and two-thirds of the total length of the shaft, simply finding the centroid of the proximal and the distal portions of the shaft would not make sense, as the points would lie at one-quarter and three-quarters of the total length of the shaft.

In this case, the solution found was to retrieve the maximum and minimum z-coordinate points of the selection made on the model's mesh, in case of the proximal and distal ends respectively, and getting the total length of the shaft. With this total length, the z-coordinate at one-third and two-thirds of the total length can be easily found. For each z-coordinate, a plane that intersects the model in a perpendicular way is created. The points on the model that intersect with the plane were obtained by using the *SectionPoints* class. Finally, the centroid method is applied to this set of points.

All the other points have the particularity of having either the maximum or the minimum value in one coordinate in their respective bone section (or of a limited zone on the bone). For instance, the most distal lateral and medial points on the Femur are the points with the lowest z-coordinates on the distal Femur.

In this way, for each of these points, an algorithm that iterates trough all the points inside a user-defined *Bouding Box* finds the needed point at the maximum or minimum value on the specified axis. The algorithm would begin at a starting point, and, if the specified condition for that specific point was fulfilled, the coordinates of the point were overwritten by the coordinates of the examined point.

One last point, the center of the knee joint, could only be found after the points in the intercondylar tubercles were found, since these two points were necessary to create a line between them, of which the medial point was found and projected on the model, in a similar fashion of the center of intercondylar fossa notch and of the center of the inferior articular surface. This process is, however, performed in a fully automatic way after the points in the intercondylar tubercles are found.

With all the landmarks defined, the program can then calculate the angles. Using the coordinates of the landmarks, vectors are formed and the angles are calculated using the generic formula on Equation 6.2, that was adapted to every angle with the needed vectors.

(6.2)
$$\varphi = arccos\left(\frac{\overrightarrow{v_1} \circ \overrightarrow{v_2}}{|v_1| * |v_2|}\right) * \frac{360}{2\pi}$$

Finally, the program is ready to print a report with the coordinates of every point and with all the calculated angles.

6.4. GRAPHICAL USER INTERFACE

As can be easily perceived, the program is dependent on user input and is supposed to be very interactive. Therefore, the graphical user interface and the user experience had to be accounted for, and its development was actually the hardest part of the program to implement. The next section is dedicated to this part of the program.

The purpose of implementing a graphic user interface, besides making the program easier to use by any user, was also to provide the user with the best tools possible to make landmark selection easier and faster.

Once the script is executed in *Geomagic*, a message appears on the output window telling the user to select the model on which he wishes to work on. A new window also appears where the file with the *wrp* file containing the model can be selected. Note that, while a patient's data is usually composed of all the bones of the two legs, the program is able to open and work in any set of bones, complete or incomplete, as long as they are properly named.

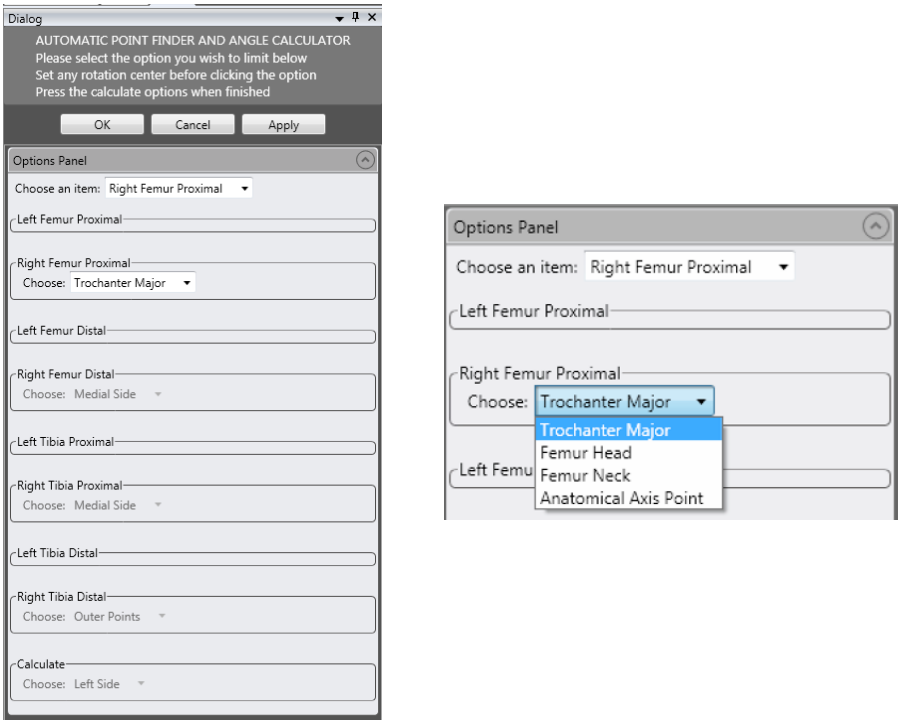

Figure 6.8. User interface displayed to the user (Left) and an example of the selectable options for a bone section (Right).

After loading the model, the program displays the model and a dialog window. An example can be seen in Figure 6.8. After some quick instructions that are to be always on display to the user, an "Options Panel" is presented with multiple clickable and interactive features.

The "Choose an item:" tab presents a drop down list of all the different bones on which the program can be used. All the possible options are: Left Femur Proximal, Right Femur Proximal, Left Femur Distal, Right Femur Distal, Left Tibia Proximal, Right Tibia Proximal, Left Tibia Distal, Right Tibia Distal and Calculate. If a bone or bone section is not available, i.e., if the model does not include the representation of a possible option, the corresponding option is not available.

Under the tab, several frames with the names of the different bones exist. The frames are always present, whether the corresponding bone section is available for selection or not. However, the user is only presented with options inside the frame if the bone is available. In the example given in Figure 6.8, the model only included the bones of the right leg, therefore all the frames for the left side bones are empty. In Figure 6.8, an example is given of the available options in a frame. Once one of these options is selected, the user must click on "Apply" and follow the instructions displayed on the screen.

The options available in each frame depend on the bone. They generally refer to the areas where the points they are related to are located. All the available options are listed below, as well as the further steps they require to work. After the user performs the steps of each option, he must always press *Apply* in the Dialog.

- ***Trochanter Major***: available in the Left Femur Proximal and Right Femur Proximal options, it allows finding the Apex/Top of the Greater Trochanter point. It requires the user to select two points in this area, close to the top. After clicking the two points, the desired point is immediately presented.

- ***Femur Head***: also available in the Left Femur Proximal and Right Femur Proximal options, it allows finding the point in the center of the Femur head, so this area should be limited. The point can be found using two different methods: either by using 4 points around the Femur Head that must be picked by the user, or by using a user created selection of the Femur Head. In Figure 6.9, the method selection menu that is presented to the user and an example of a selection made while using the second method is shown. After both methods, the point is then presented.

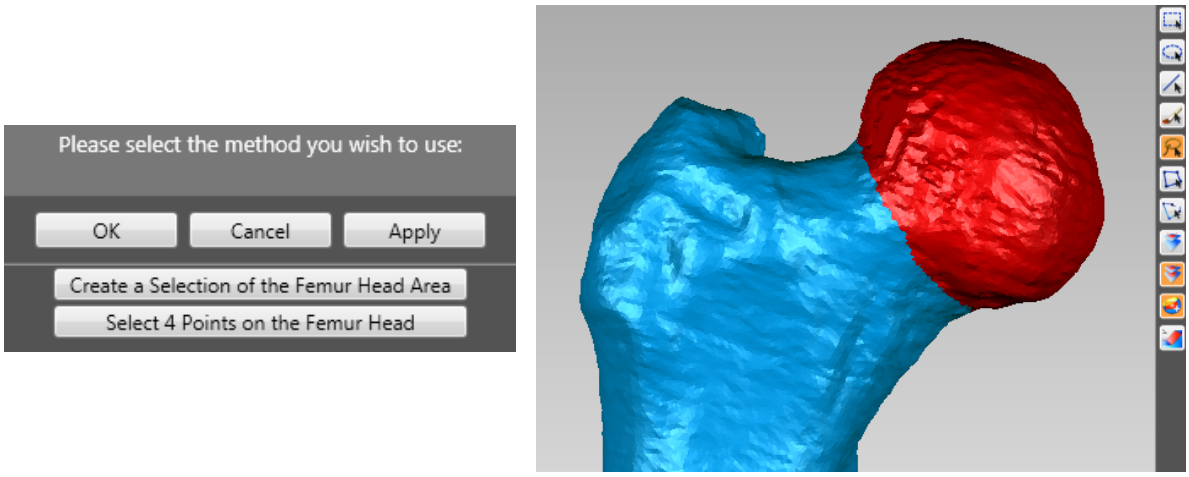

Figure 6.9. Method selection displayed to the user (Left) and an example of a user's Femur Head selection (in red) (Right).

- ***Femur Neck***: another option only available in the Left Femur Proximal and Right Femur Proximal options, it allows finding the point in the center of the Femur Neck, so this area should be limited by the user, as can be seen in Figure 6.10. The user then gets the point presented in the model.

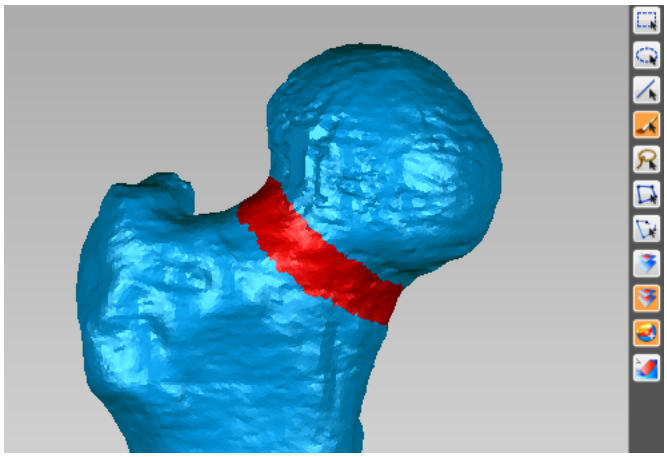

Figure 6.10. Example of a user's Femur Neck selection (in red).

- ***Anatomical Axis Point***: this option's goal is to find a central point in the bone shaft which will be then used to define the bone axis. It uses a user created selection of a portion of the shaft. It is important to differentiate if a Torsion CT is being used or not, since the user selection must be different for the two cases, as can be seen on Figure 6.11. This option is present in every bone section and it results in four distinct points for one whole leg: two Proximal Point Center of Shaft and two Distal Point Center of Shaft, one of each for the Femur and then the Tibia.

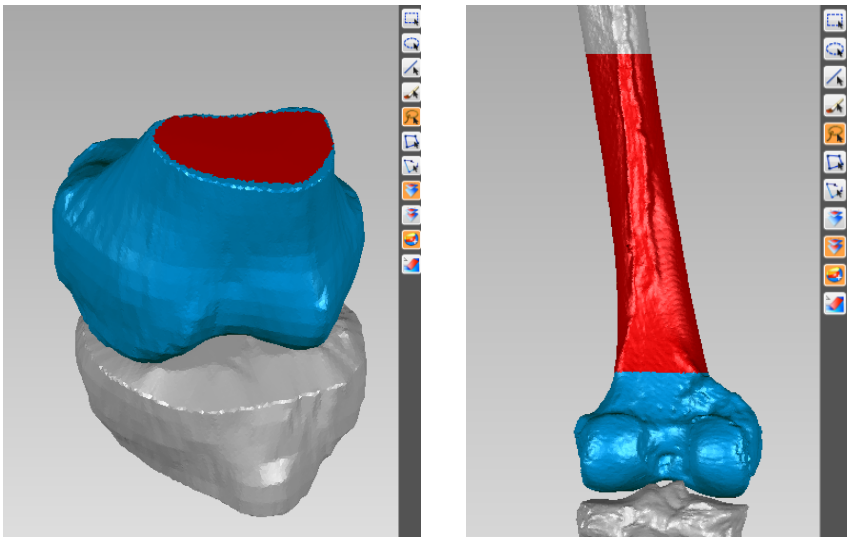

Figure 6.11. Example of user's selections (in red) for the Right Tibia Distal, in a Torsion CT (Left) and a normal CT (Right).

- ***Medial Side*** (Femur Distal): this option, in the Left Femur Distal and the Right Femur Distal, allows finding all the Femur Distal anatomical points that are found on the medial side by asking the user to select two points in this side of the bone by clicking. This option results in two different points that are presented to the user after the two clicks.

- ***Lateral Side*** (Femur Distal): complementing the previous, this option, in the Left Femur Distal and the Right Femur Distal, allows the user to find the Femur Distal anatomical points that lay on the lateral side by once again asking the user to select two points in this side of the bone by clicking. This option results in two different points that are presented to the user after the two clicks.

- ***Intercondylar Notch***: available in both Left Femur Distal and Right Femur Distal, this option allows the user to find the middle point of the Intercondylar Notch Area, so this area should be limited. It uses a user created selection of the Intercondylar Notch Area, as can be seen in Figure 6.12.

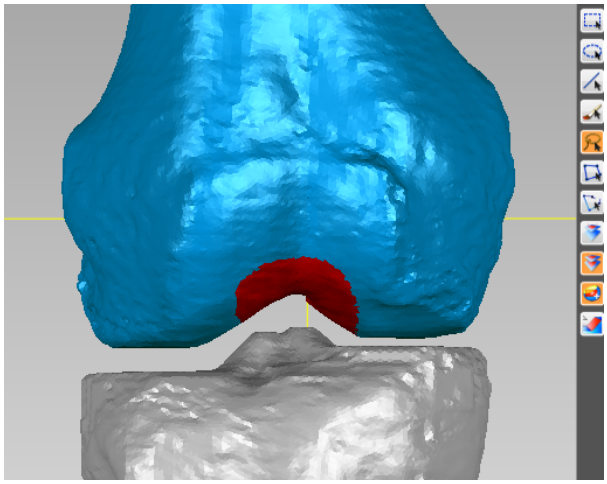

Figure 6.12. Example of a user's Intercondylar Notch selection (in red) on the Right Femur Distal.

- ***Medial Side*** (Tibia Proximal): this option, in the Left Tibia Proximal and the Right Tibia Proximal, allows finding all the anatomical points that are located on the medial side of the Tibia Proximal. It uses a user created selection of the Medial Side of the Tibial Plateau, as can be seen in Figure 6.13. After selecting the area, the user is also asked to click on two different points of the selection, creating four points from this selection automatically.

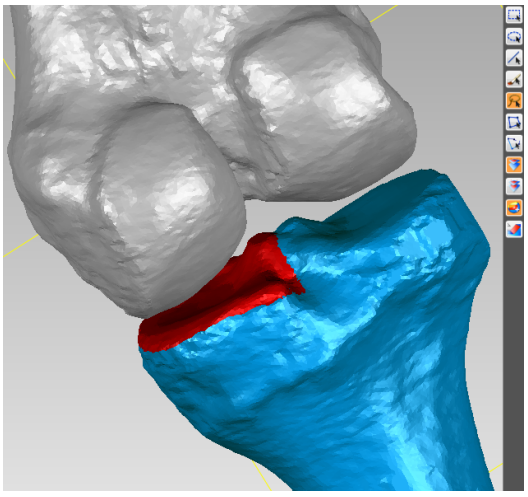

Figure 6.13. Example of a user's Medial Side selection (in red) on the Right Tibia Proximal.

- ***Lateral Side*** (Tibia Proximal): as the previous option, this one allows finding all the Tibia Proximal anatomical points that are located on the lateral side of the bone. It also asks for a user created selection of the Lateral Side of the Tibial Plateau which is then followed by a request to click on two points on the model. This option creates four different points as well.

- ***Outer Points***: it allows finding the Outer Points, Lateral and Medial, of both Left Tibia Distal and Right Tibia Distal. It requires the user to create a selection of both the Malleolus of the Tibia, as the example in Figure 6.14. The program then creates the two points from this selection.

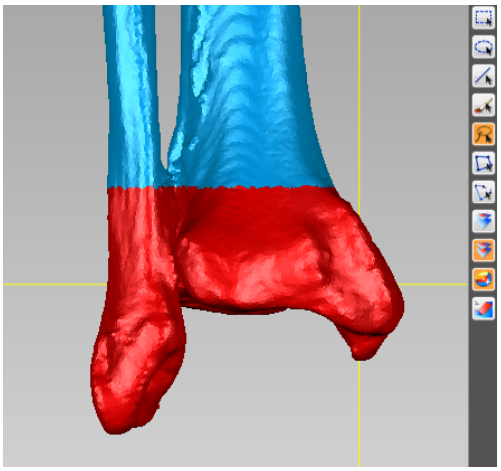

Figure 6.14. Example of a user's Outer Points selection (in red) on the Right Tibia Distal.

- ***MPTBA***: this last option allows finding the Middle Point of the Tibia Bearing Area, by requesting the user to create a selection of the Tibia Bearing Area to then present the point automatically. An example of the needed selection can be seen in Figure 6.15.

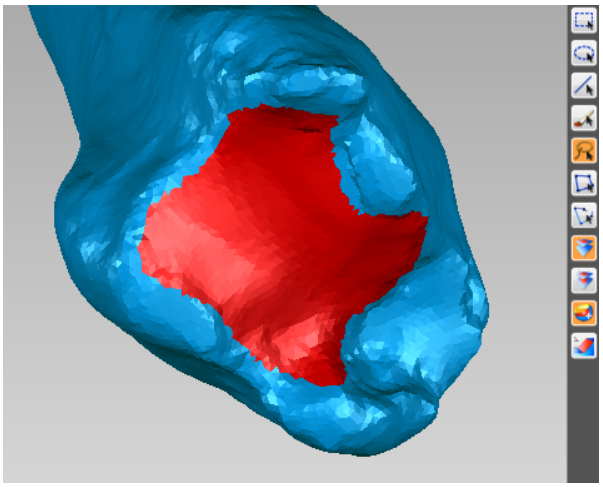

Figure 6.15. Example of a user's MPTBA selection (in red) on the Right Tibia Proximal.

Besides all these options, there are also three auxiliary buttons available at the bottom of the Dialog on Figure 6.8, two of which can prove to be extremely useful: a "Delete Recent" button, which allows the user to delete the latest points added by one of the options listed below, in case he finds the points not satisfactory, and a "Delete All" button, which deletes every single point found up to the moment the button is pressed. The other button allows the user to alternate between the program settings needed for a Torsion CT and a normal CT, and it is used when needed for the "Anatomical Axis Point" option. The looks of these buttons can be seen in Figure 6.16.

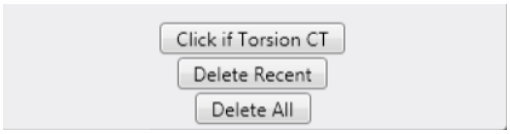

Figure 6.16. Auxiliary buttons available on the User Interface.

The finished result on the 3D model looks like the example in Figure 6.17.

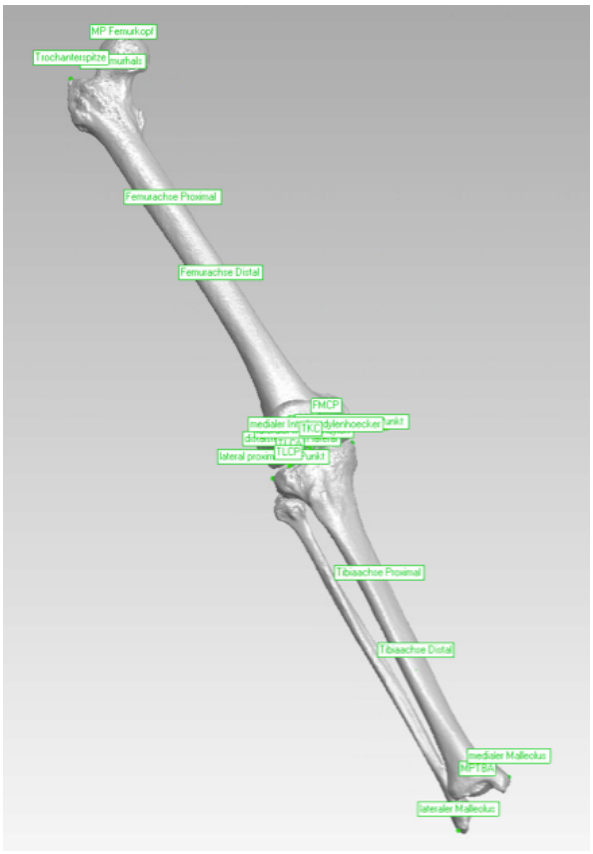

Figure 6.17. Example of a 3D model after finding every landmark.

Once all the points for one leg have been found, the user can proceed to calculate the angles. In order to do that, he must select the option “Calculate” under the “Choose an item:” tab. The user must then select which side he wishes to calculate and press *Apply*. A new window appears on the screen and the user must choose a *.txt* file in which he wishes to save the results of the calculations.

The saved *txt* file contains all the results from the program: first, the side which was calculated is presented, followed by the 3D coordinates of all the points the program has found and lastly it provides the results of the calculation.

7. PROGRAM TESTING

The International Software Testing Qualifications Board (ISTQB), the world-wide leader in the certification of competences in software quality assurance, defines quality as “the degree to which a component, system or process meets specified requirements and/or user/customer needs and expectations”. More specifically, it defines software quality as “the totality of functionality and features of a software product that bear on its ability to satisfy stated or implied needs”. The Institute of Electrical and Electronics Engineers (IEEE), the world's largest association of technical professionals and well known among engineers, also defines quality as “the degree to which a system, component, or process meets specified requirements and meets customer or user needs or expectations”.

These definitions are, nevertheless, quite generic. The degree of compliance to the requirements and the customer/user needs and expectations must be measured in order to evaluate the quality level of a software. This is done trough the individual evaluation of the different dimensions of software quality. Some of these dimensions can also be used to compare the software to other processes used for the same end.

Accuracy, the quality of being correct or precise, is a very important dimension. An accurate program must be one that is reliable when the same process, in this case, measurements, are repeated one or more times by the same user (intraobserver reliability) or for different users performing the same measurements (interobserver reliability). Therefore, tests must be performed to make sure the program can be considered accurate in both cases, validating it as able to perform an accurate alignment assessment.

Another very important, if not the most important, dimension is functionality, which can be described as the ability of a software to carry out the functions as specified or desired. In this case, testing for functionality is to test if the program can perform a correct assessment, with values that match those a medical doctor would get on his own. In this sense, a test that compares the program’s findings with manual findings, particularly the ones of trained medical doctors that are used to perform this alignment assessment on a daily basis, is vital.

The ability of a software system to achieve a certain result without wasted resources can be described as a program’s efficiency. Time is a very important resource that is part of the efficiency dimension. A time-efficient software is one that performs a certain task that can be done in a variety of ways in the fastest way possible. In the alignment assessment scenario, developing a time-efficient tool is developing a program that significantly reduces the time necessary to perform the assessment task in its fullness. A test that compares the time needed by the program with the time needed to do the same task manually is then necessary.

7.1. Intraobserver Reliability Testing

7.1.1. Method

In order to assure the intraobserver reliability of the program, the same user must obtain the same results every time the program is run for the same patient. Therefore, for this test, the same user was asked to run the 3D calculation program six times for each leg of Patient 1.

The mean, the standard deviation and the mean absolute deviation (M.A.D.) were calculated so that the results can be more objectively compared.

7.1.2. Results

In Table 7.1 the automatic 3D results for the left leg calculations are presented, while in Table 7.2 the results for the right leg are presented.

Table 7.1. Intraobserver results of the automatic 3D calculation for the left leg of Patient 1.

PATIENT 1 - LEFT LEG									
Measures	AUTOMATIC								
	1st Run	2nd Run	3rd Run	4th Run	5th Run	6th Run	Mean	St. Deviation	M.A.D.
HKA (º)	178.53	178.35	178.27	178.35	178.35	178.21	178.34	0.11	0.07
MAD (mm)	5.08	5.70	5.99	5.70	5.07	6.16	5.62	0.46	0.36
FTA (º)	48.41	49.22	56.17	50.80	53.76	45.18	50.59	3.93	2.99
Position of the Condyles (º)	174.95	174.95	174.95	174.95	174.95	174.95	174.95	0.00	0.00
TTA (º)	10.87	13.70	10.16	15.07	14.18	10.59	12.43	2.13	1.89
Position of the Malleoli (º)	158.13	158.13	158.13	158.13	158.13	158.13	158.13	0.00	0.00
LPFA (º)	93.53	93.24	92.76	95.12	95.37	95.36	94.23	1.18	1.05
mLDFA (º)	89.13	90.03	89.37	87.47	88.87	87.01	88.65	1.16	0.94
MPTA (º)	93.19	92.82	93.25	93.87	93.85	93.19	93.36	0.42	0.33
MPFA (º)	100.60	100.55	100.05	102.32	102.12	102.51	101.36	1.07	0.96
CCD (º)	130.00	130.86	129.30	132.06	135.34	126.68	130.71	2.90	2.05
Medial Tibial Slope (º)	80.13	77.76	80.60	77.59	79.29	80.77	79.36	1.40	1.14
Lateral Tibial Slope (º)	80.07	78.13	77.25	78.02	79.25	79.12	78.64	1.02	0.84

Table 7.2. Intraobserver results of the automatic 3D calculation for the right leg of Patient 1.

PATIENT 1 - RIGHT LEG									
Measures	**AUTOMATIC**								
	1st Run	**2nd Run**	**3rd Run**	**4th Run**	**5th Run**	**6th Run**	**Mean**	**St. Deviation**	**M.A.D.**
HKA (º)	179.02	178.92	178.98	178.95	178.97	178.89	178.96	0.05	0.04
MAD (mm)	3.37	3.69	3.49	3.60	3.54	3.8	3.58	0.15	0.12
FTA (º)	49.93	49.04	47.59	45.66	44.72	47.28	47.37	1.97	1.48
Position of the Condyles (º)	168.85	168.85	168.85	168.85	168.85	168.85	168.85	0.00	0.00
TTA (º)	5.80	7.05	7.50	6.50	3.35	6.55	6.13	1.47	1.03
Position of the Malleoli (º)	160.82	160.82	160.82	160.82	160.82	160.82	160.82	0.00	0.00
LPFA (º)	94.47	95.07	95.04	93.97	95.04	94.54	94.69	0.44	0.36
mLDFA (º)	82.96	83.06	84.17	83.08	83.31	82.77	83.23	0.50	0.34
MPTA (º)	93.16	92.61	92.93	92.92	93.44	93.34	93.07	0.31	0.25
MPFA (º)	102.45	102.11	102.15	101.06	102.21	101.79	101.96	0.49	0.36
CCD (º)	134.58	133.85	132.11	130.42	129.40	131.75	132.02	1.97	1.50
Medial Tibial Slope (º)	79.95	79.48	78.66	80.02	80.08	80.02	79.70	0.56	0.42
Lateral Tibial Slope (º)	80.79	76.34	79.52	79.57	77.91	77.97	78.68	1.58	1.28

7.1.3. ANALYSIS

The purpose of this test was to assure the program is reliable when the same measurements are repeated multiple times by the same user, in this case, six times for each leg. In this way, only the variability of the results is to be analyzed.

In both legs, the values for the FTA, TTA and CCD are the ones that display higher standard deviation and mean average deviation values, with the deviations being smaller on the right leg.

The rest of the measurements present small deviations, with approximately half of them even presenting less than 0.5º or 0.5 mm of deviation, which can be considered small deviation values.

7.2. INTEROBSERVER RELIABILITY TESTING

7.2.1. METHOD

In order to assure the interobserver reliability of the program, different users must obtain the same results every time the program is run for the same patient. Therefore, for this test, three different users, with different levels of expertise and familiarization with the program, were asked to run the 3D calculation program for Patient 1. In this test, User 1 is a trained orthopedic surgeon with no previous familiarization with the program, User 2 is a medicine student that has been exposed to the program and User 3 is a engineering student with a lot of practice using the program. All users used the same model.

Once again, the mean, the standard deviation and the M.A.D. were calculated so that the results can be more objectively compared.

7.2.2. RESULTS

In Table 7.3 the automatic 3D results for the left leg calculations are presented, while in Table 7.4 the results for the right leg are presented.

Table 7.3. Interobserver results of the automatic 3D calculation for the left leg of Patient 1.

PATIENT 1 - LEFT LEG						
Measures	**AUTOMATIC**					
	User 1	**User 2**	**User 3**	**Mean**	**St. Deviation**	**M.A.D.**
HKA (º)	178.46	178.34	178.37	178.39	0.06	0.05
MAD (mm)	5.33	5.74	5.61	5.56	0.21	0.15
FTA (º)	45.74	47.61	50.35	47.90	2.32	1.63
Position of the Condyles (º)	174.95	174.95	174.95	174.95	0.00	0.00
TTA (º)	11.71	15.43	15.51	14.22	2.17	1.67
Position of the Malleoli (º)	158.13	158.13	158.13	158.13	0.00	0.00
LPFA (º)	94.25	93.34	93.9	93.83	0.46	0.33
mLDFA (º)	89.80	90.43	88.60	89.61	0.93	0.67
MPTA (º)	92.62	99.26	93.87	95.25	3.53	2.67
MPFA (º)	101.59	100.8	101.12	101.17	0.40	0.28
CCD (º)	126.61	128.83	131.68	129.04	2.54	1.76
Medial Tibial Slope (º)	76.4	76.37	78.18	76.98	1.04	0.80
Lateral Tibial Slope (º)	77.26	77.52	76.76	77.18	0.39	0.28

Table 7.4. Interobserver results of the automatic 3D calculation for the right leg of Patient 1.

PATIENT 1 - RIGHT LEG						
Measures	**AUTOMATIC**					
	User 1	**User 2**	**User 3**	**Mean**	**St. Deviation**	**M.A.D.**
HKA (º)	179.38	179.08	179.02	179.16	0.19	0.15
MAD (mm)	2.13	3.15	3.37	2.88	0.66	0.50
FTA (º)	45.48	45.7	49.93	47.04	2.51	1.93
Position of the Condyles (º)	168.85	168.85	168.85	168.85	0.00	0.00
TTA (º)	6.48	8.28	5.80	6.85	1.28	0.95
Position of the Malleoli (º)	160.82	160.82	160.82	160.82	0.00	0.00
LPFA (º)	95.68	94.23	94.47	94.79	0.78	0.59
mLDFA (º)	86.44	85.84	82.96	85.08	1.86	1.41
MPTA (º)	93.41	92.39	93.16	92.99	0.53	0.40
MPFA (º)	102.72	101-40	102.45	102.59	0.19	0.13
CCD (º)	129.45	130.24	134.58	131.42	2.76	2.10
Medial Tibial Slope (º)	79.23	78.17	79.95	79.12	0.90	0.63
Lateral Tibial Slope (º)	80.91	79.74	80.79	80.48	0.64	0.49

7.2.3. ANALYSIS

The purpose of this test was to assure the program is reliable for different users performing the same measurements, in this case, the measurements for both legs of Patient 1. In this way, only the variability of the results is to be analyzed.

As with the intraobserver results, the values for the FTA, TTA and CCD display high standard deviation and mean average deviation values. However, for the left leg, MPTA is the value with the highest deviation values in this test (3.53º for the standard deviation and 2.67º for the M.A.D.), while, for the intraobserver results or for the right leg, the deviation was, respectively, below/around 0.5º. For the right leg, it's actually the deviation values for the mLDFA that stand out, but not as much as the previously pointed out measurements.

The rest of the measurements present small deviations once again, with almost all of them having less than 0.5º or 0.5 mm of deviation, which can be considered small deviation values.

7.3. FUNCTIONALITY TESTING

7.3.1. METHOD

In order to assure the functionality of the program, the program's automatic findings must match manual findings, i.e. the angles and measurements that result from the landmarks automatically found by the program must match those that result from landmarks set manually, particularly by trained medical doctors that possess knowledge of the human anatomy.

For this test, the same users who performed the interobserver test were asked to manually locate the landmarks for Patient 1 and then perform the 3D calculation. The interobserver setting was chosen since the chances for variability are higher than in a intraobserver setting. The mean, the standard deviation and the M.A.D. of the manual findings are compared to those of the automatic findings and to the expected values according to the literature. All users used the same model once again.

7.3.2. RESULTS

In Table 7.5 the manual 3D results for the left leg calculations are presented, while in Table 7.6 the manual results are compared to the automatic ones and to the expected values. In turn, Tables 7.7 and 7.8 refer to the right leg.

Table 7.5. Interobserver results of the manual 3D calculation for the left leg of Patient 1.

PATIENT 1 - LEFT LEG						
Measures	**MANUAL**					
	User 1	**User 2**	**User 3**	**Mean**	**St. Deviation**	**M.A.D.**
HKA (º)	178.43	178.65	178.58	178.55	0.11	0.08
MAD (mm)	5.46	4.69	4.91	5.02	0.40	0.29
FTA (º)	45.51	47.42	45.77	46.23	1.04	0.79
Position of the Condyles (º)	169.96	169.90	169.94	169.93	0.03	0.02
TTA (º)	20.55	18.47	23.34	20.79	2.44	1.70
Position of the Malleoli (º)	160.99	161.97	161.36	161.44	0.49	0.35
LPFA (º)	88.96	89.44	87.28	88.56	1.13	0.85
mLDFA (º)	87.73	85.60	86.71	86.68	1.07	0.72
MPTA (º)	91.99	92.49	91.58	92.02	0.46	0.31
MPFA (º)	96.98	96.85	94.94	96.26	1.14	0.88
CCD (º)	125.02	127.06	125.90	125.99	1.02	0.71
Medial Tibial Slope (º)	78.83	79.51	77.00	78.45	1.30	0.96
Lateral Tibial Slope (º)	79.98	79.17	78.59	79.25	0.70	0.49

Table 7.6. Comparison of the interobserver results and the expected values for the left leg of Patient 1.

PATIENT 1 - LEFT LEG							
Measures	**MANUAL**			**AUTOMATIC**			**Expected Values**
	Mean	**St. Deviation**	**M.A.D.**	**Mean**	**St. Deviation**	**M.A.D.**	
HKA (º)	178.55	0.11	0.08	178.39	0.06	0.05	180º
MAD (mm)	5.02	0.40	0.29	5.56	0.21	0.15	0
FTA (º)	46.23	1.04	0.79	47.90	2.32	1.63	24.1 ± 17.4°
Position of the Condyles (º)	169.93	0.03	0.02	174.95	0.00	0.00	-
TTA (º)	20.79	2.44	1.70	14.22	2.17	1.67	34.9 ± 15.9 °
Position of the Malleoli (º)	161.44	0.49	0.35	158.13	0.00	0.00	-
LPFA (º)	88.56	1.13	0.85	93.83	0.46	0.33	90.0 ± 5.0°
mLDFA (º)	86.68	1.07	0.72	89.61	0.93	0.67	87.5 ± 2.5 °
MPTA (º)	92.02	0.46	0.31	95.25	3.53	2.67	87.5 ± 2.5 °
MPFA (º)	96.26	1.14	0.88	101.17	0.40	0.28	83.0 ± 5.0°
CCD (º)	125.99	1.02	0.71	129.04	2.54	1.76	130 ± 5.0°
Medial Tibial Slope (º)	78.45	1.30	0.96	76.98	1.04	0.80	80.5 ± 3.5°
Lateral Tibial Slope (º)	79.25	0.70	0.49	77.18	0.39	0.28	80.5 ± 3.5°

Table 7.7. Interobserver results of the manual 3D calculation for the right leg of Patient 1.

PATIENT 1 - RIGHT LEG						
Measures	**MANUAL**					
	User 1	**User 2**	**User 3**	**Mean**	**St. Deviation**	**M.A.D.**
HKA (º)	179.50	178.83	178.70	179.01	0.43	0.33
MAD (mm)	1.73	4.03	4.50	3.42	1.48	1.13
FTA (º)	43.65	49.24	48.11	47.00	2.96	2.23
Position of the Condyles (º)	4.91	4.15	6.61	5.22	1.26	0.92
TTA (º)	22.41	33.46	21.89	25.92	6.54	5.03
Position of the Malleoli (º)	24.45	38.01	21.28	27.91	8.89	6.73
LPFA (º)	92.89	89.95	89.34	90.73	1.90	1.44
mLDFA (º)	84.57	82.82	81.81	83.07	1.40	1.00
MPTA (º)	91.39	91.49	91.49	91.46	0.06	0.04
MPFA (º)	101.43	97.41	96.19	98.34	2.74	2.06
CCD (º)	122.86	131.23	128.35	127.48	4.25	3.08
Medial Tibial Slope (º)	78.15	79.79	78.78	78.91	0.83	0.59
Lateral Tibial Slope (º)	78.93	79.94	80.92	79.93	1.00	0.67

Table 7.8. Comparison of the interobserver results and the expected values for the right leg of Patient 1.

PATIENT 1 - RIGHT LEG							
Measures	**MANUAL**			**AUTOMATIC**			**Expected Values**
	Mean	**St. Deviation**	**M.A.D.**	**Mean**	**St. Deviation**	**M.A.D.**	
HKA (º)	179.01	0.43	0.33	179.16	0.19	0.15	180º
MAD (mm)	3.42	1.48	1.13	2.88	0.66	0.50	0
FTA (º)	47.00	2.96	2.23	47.04	2.51	1.93	24.1 ± 17.4°
Position of the Condyles (º)	5.22	1.26	0.92	168.85	0.00	0.00	-
TTA (º)	25.92	6.54	5.03	6.85	1.28	0.95	34.9 ± 15.9 °
Position of the Malleoli (º)	27.91	8.89	6.73	160.82	0.00	0.00	-
LPFA (º)	90.73	1.90	1.44	94.79	0.78	0.59	90.0 ± 5.0°
mLDFA (º)	83.07	1.40	1.00	85.08	1.86	1.41	87.5 ± 2.5 °
MPTA (º)	91.46	0.06	0.04	92.99	0.53	0.40	87.5 ± 2.5 °
MPFA (º)	98.34	2.74	2.06	102.59	0.19	0.13	83.0 ± 5.0°
CCD (º)	127.48	4.25	3.08	131.42	2.76	2.10	130 ± 5.0°
Medial Tibial Slope (º)	78.91	0.83	0.59	79.12	0.90	0.63	80.5 ± 3.5°
Lateral Tibial Slope (º)	79.93	1.00	0.67	80.48	0.64	0.49	80.5 ± 3.5°

7.3.3. ANALYSIS

The purpose of this test was to compare the program's findings to those of a manual approach, in this case, the measurements for both legs of Patient 1, in a interobserver setting. It is also relevant to analyze how these sets of data compare to the expected values according to the literature.

In both legs, the values for HKA are very similar in both manual and automatic assessments, with the latter having smaller deviation values. The values for MAD are not as similar, but the automatic assessment presents smaller deviations values as well. Also, unlike for the automatic results for the Position of the Condyles and the Position of the Malleoli, the manual results for both legs do not present zero deviation as the automatic results do. Furthermore, the deviation value for the Position of the Malleoli on the manually assessed right leg is the highest recorded.

The deviation values for MPTA are higher for both legs on the automatic results, particularly on the left leg. The deviation values that stand out on the automatic results for the right leg are the ones for the mLDFA and Medial Tibial Slope, even though the difference to the manual results is small.

Differences arise between legs on the FTA and CCD measurements, where, on the left leg, they present higher deviation values for the automatic assessment, whereas on the right, they present lower deviation values when compared to the manual assessment.

When comparing both manual and automatic findings to the expected values, both FTA and TTA stand out as being far from what was expected on both types of assessment. Nevertheless, the manual and automatic mean values for the found FTA measurements are similar in both legs and the ones for the TTA measurement are similar on the left leg.

Also far from what was expected, but not as significantly, are the assessed values for the MPTA and MPFA on both legs. However, the manual and automatic mean values are actually approximate in both legs.

All the other measurements, manual and automatic, can be considered quite similar to the expected values and similar amongst themselves, with the exception of the values found for the Position of the Condyles and the Position of the Malleoli on the right leg, where, while there is no expected value for comparison, the manual mean value is very different from the automatic mean value.

7.4. Time Efficiency Testing

7.4.1. Method

In order to assure the developed program is more time efficient than manually performing the alignment assessment, the time it took each user to perform their task on the two previous tests was being recorded for comparison. The mean is calculated for an easier overall comparison.

7.4.2. Results

In Table 7.9, the recorded times for the manual and automatic alignment assessments for Patient 1 are presented.

Table 7.9. Comparison of the times for the interobserver manual and automatic results of Patient 1.

Assessment	Left Leg			Right Leg			Mean
	User 1	User 2	User 3	User 1	User 2	User 3	
Manual	12:25.000	12:19.140	12:22.160	12:19.580	12:18.190	12:18.270	12:20.390
Automatic	12:50.720	08:59.230	05:55.590	08:15.830	07:19.510	06:58.510	08:23.232

7.4.3. Analysis

Comparing the means, the automatic assessment immediately reveals itself to be faster than the manual assessment, even though not very significantly.

The time needed for the manual assessment is very approximate in all cases. However, the time difference between the two types of assessment is very different from user to user, with User 3 being the fastest, and User 1 being the slowest while performing the automatic assessment.

7.5. Discussion of the Results

As previously stated in Chapter 4, the final objective, after the development stage, was to ensure that the program is reliable and consistent in its results in both intraobserver and interobserver domain and that it can replicate the manual assessment by comparing the results obtained by using the program with manual assessment results. For this reason, four different tests were performed and their results, along with a quick analysis, have already been presented. Now, it is relevant to further analyze and discuss these results, in a particular way and in a more general context of the program, to ascertain if the final objective was met.

When analyzing the intraobserver reliability testing results, the FTA, TTA and CCD angles stood out as having big deviation values. This was also verified in the interobserver reliability testing. In addition, the found values for the FTA and TTA angles do not match the expected values according to the literature (the values for the CCD match the expected values), in both automatic and manual findings.

Since the same formulas are used in each run, the source of variability in these measurements must be the landmarks found by the program. The landmarks involved in these measurements are: the center of the femur head, the center of the femur neck, the proximal point and distal point of the center of the femur shaft, the most posterior points of the lateral and medial condyles of the femur, the most posterior points of the lateral and medial condyles of the tibia, the most medial point of the medial malleolus and, finally, the most lateral point of the lateral malleolus.

From this list of landmarks, due to the process by which they are found, the ones that are the least likely to be the source of the variability are the most posterior points of the lateral and medial condyles of the femur, the most medial point of the medial malleolus and the most lateral point of the lateral malleolus.

The variability in the FTA values is most likely due to the point in the center of the femur neck, since its location is very dependent on the area selected by the user. The same can be said about the the most posterior points of the lateral and medial condyles of the tibia, which are, in turn, the most likely source of variability in the TTA. As for the source of variability in the CCD values, besides the fact that it also uses the center of the femur neck landmark, the proximal point and distal point of the center of the femur shaft can also suffer from some sort of user selection variability, even though this is less likely, as the point will always lie in the center of the shaft, they just might not be precisely at one-third and two-thirds of the shaft.

Also, the deviations found for the MPTA are once again most likely explained by the high dependency on the area selected by the user to find the the most proximal and lateral point of the Tibia plateau and the most proximal and medial point of the Tibia plateau landmarks.

Since every user was free to use the program as they saw fit, it is not possible to infer the variability caused by the center of the femur head, as each run might have used a different method to locate this point. Nevertheless, using the selection method may be a cause of variability, as in the cases mentioned before and this may actually explain the deviation values found for the mLDFA on the right leg.

Nonetheless, the issues with the MPTA and mLDFA are only found on one leg (each), so more information should be collected before conclusions can be drawn, i.e. more patients should be analyzed. An increase in the sample size shall bring more insight on this matter and the observed variations can even be exclusive to this patient.

As for why the found values for the FTA and TTA angles do not match the expected values according to the literature on both automatic and manual assessments, the explanation might be simple: the expected values come from a 2D calculation and not a 3D one. The extent to which this is the absolute reason is not certain.

Firstly, one can notice that the manual and the automatic values for the FTA on both legs are very close, so both methods are producing approximately the same calculated angles (considering the mean values), so it is more of a calculation problem (which can involve the used landmarks or the algorithm itself) than it is of a landmark finding problem. Nevertheless, an exact reason for this error cannot be found.

Secondly, when it comes to the difference of the manual and the automatic values for the TTA to the expected values (and also among themselves), an explanation can be presented, which is that the necessary points are difficult to be precisely located, both by the program and the methods it uses, and by the user performing a manual assessment using a 3D model and using the *Geomagic* software. Locating these landmarks using the defined methodologies in the exact locations as they should be in is a very hard task, particularly for the automatic method.

In the functionality testing results, the assessed values for the HKA, MAD, the Position of the Condyles and the Position of the Malleoli stand out, since they match both manually obtained values and the expected values (when applicable). The HKA and MAD are core measurements of the alignment assessment and it can be said that the developed program is properly calculating these values.

Finally, the results for the time efficiency testing don't come across as impressive at a glance, but the presented values can also be explained by the problem of the sample size. Only one run per user and per leg is available and if one takes into account the fact that there are different levels of familiarity with the developed program among the users, the small difference between the average time for the manual and automatic assessment is explained.

If User 3, the most experienced user regarding the automatic assessment, can be taken as example, the program allows for an almost 50% faster alignment assessment when compared to a manual method.

7.6. Errors and Further Statistical Analysis

The error, in statistics, is the amount by which an observation differs from its expected value, and it is a very common statistical concept. The error in a study can be caused by different sources and how each source contributes to the final error might be evaluated, resulting in a final value for the error (which is always, nonetheless, an approximation).

In the medical field, the assessment of the error is of extreme importance as it acts as a guarantee that the drug, treatment method, device or software is effective in what it is supposed to to, carrying the smallest chance possible of anything going wrong while using it.

As the developed software aims at clinical application, assessing the error associated with its validation is very important, as it influences the perceived reliability of the software and calls into question its usability in the clinical context it is supposed to be used in.

In this specific case, the final statistical error associated with the results from the software testing can come from: the error associated with the imaging system used to obtain the images of the patients, the error associated with using the *Mimics* software, the error associated with using the *Geomagic* software and finally the error caused by all the human intervention during the alignment assessment procedure. Random errors can also be considered.

Finding the errors associated with the first stated source can prove to be a hard task, as the error of the images coming from an imaging system depend on which system was used, and due to the nature of the developed program, any system can be used, so no standard can be set. Also, the standard error associated with using the third-party softwares is not easy to access.

This leaves the error caused by human intervention to be determined. The intraobserver and interobserver tests that were performed, while serving as a way to validate the software, can also act as a way of setting a value of error and also trust on the program's results. A statistical study can be designed in a way so that a value of error and variation can be set.

In statistics, any study has a predetermined error margin associated with it. The smaller the margin of error, the more reliable the study and its results. Deciding on a margin error for a study envolves deciding how large a sample size needs to be in order to estimate a quantity of interest to some desired precision. So, if different error margins will require very different sample sizes.

According to [22], for a 5% margin, the desirable margin in medical statistics, the size of the sample should be 400. This means that in the intraobserver context previously explored, the same user should have performed 400 automatic assessments, and in the interobserver context, 400 different patients should have been assessed by the different users, in order to assure that the estimated values fall within 5% of their "true" error-free value. A size sample of 11 already results in an error margin as large as 30%. It is then clear that the performed tests have an enormous and unsurpassable error margin associated with them, which would classify them as unfit to any serious clinical validation study, which backs the need for an increase on sample size and further testing.

Also, another problem in reliability studies, is defining the number of users, or so-called raters, that must participate to ensure an adequate precision in the results. The coefficient of variation is a measure of relative variability widely influenced by the number of users. The more users are involved, the smaller is the chance that the variability of the results is due to them, and therefore the smaller the coefficient of variation is. For a 5% coefficient of variation, once again a target value in this type of studies, 40 different users should be involved, with an "absurdly big" 30% coefficient already requiring seven different users, which makes the three-users scenario that was used in the interobserver testing clearly insufficient.

Calculating the Interclass Correlation Coefficient, also known as the ICC, would have been more appropriate in the interobserver context, as it corresponds to the assessment of the consistency/

reproducibility of quantitative measures made by different users measuring the same quantity, describing how strongly units in the same group, or measures of the same thing, to simplify, resemble each other. It would have provided better information that the standard deviation or the M.A.D., however, statistically speaking, due to high error margin and coefficient of variation, calculating the ICC would have had little significance, resulting in the approach that was ultimately chosen and presented. With a bigger sample of patients and more users, calculating the ICC would provide more information on how reliable the developed software is.

8. LIMITATIONS AND SUGGESTIONS

During the project, several limitations became evident and they were either overcame/ eliminated, though not necessarily for a better option, or simply accepted as restrictions/flaws.

One of the initial limitations was the fact that *Geomagic Studio 14* uses the Python programming language in its scripting engine, which was a language with which I had no previous experience with. This created a number of problems and limitations: firstly, this made the development of the program slower, as learning and actual programming had to be done at the same time; secondly, it made the development of the program harder, as a lot of times there wasn't enough knowledge to fix a problem and whole new solution had to be found; and finally, it limited the options that could be used to find the landmarks, once again due to the lack of knowledge on the extent of the possibilities that Python provides.

Geomagic itself posed as a limiting factor to the development of a better program, as some "bugs" could not be surpassed. The biggest limitation was related to finding the landmarks on the proximal Tibia.

The original plan was to follow the method used on [21] to locate the landmarks that lie on the Tibia plateau, where a best fit circle to each condyle is created, as can be seen in Figure 81, and all the relevant points are located along the circle.

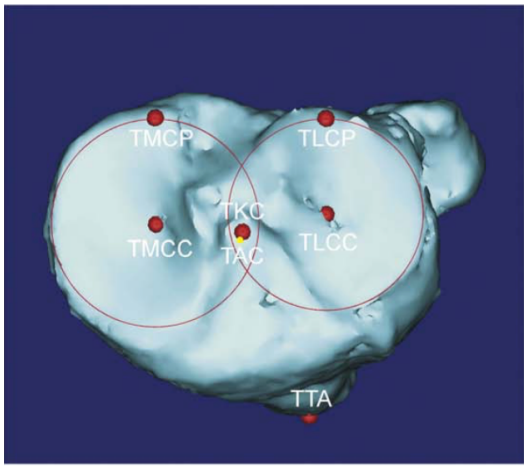

Figure 7.1. Points on the Tibia plateau obtained from best fit circles to the condyles (from [G]).

When trying to apply this methodology in *Geomagic*, while the best fit circle could easily be created, actually using it to find the points proved to be impossible. For an unknown reason, *Geomagic* would consider clearly improperly aligned vectors to be properly aligned, as can be seen in Figure 7.2, where the radial vectors marked on the circle where considered to be perfectly parallel to the x- and y-axis by the software when they are clearly not, causing the landmarks to be placed on the wrong positions, which affected the calculations.

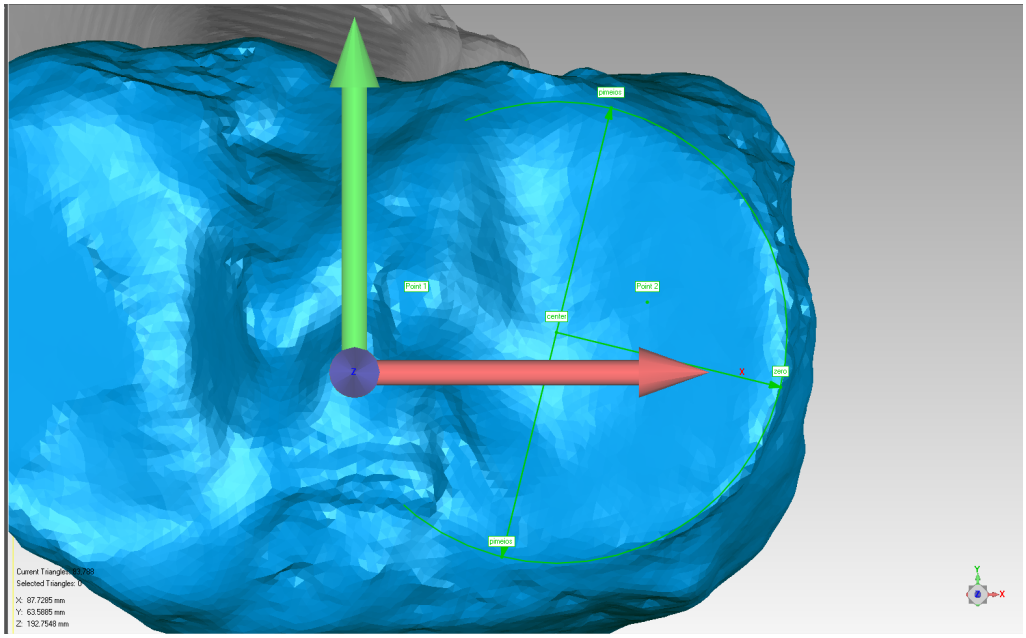

Figure 7.2. Attempt to use the best fit circle methodology to find the landmarks on the Tibia plateau.

A successful application of this method would have made finding these points less user-dependent when compared to the present method by which they are found, and this would result in less variability of the results, and therefore, in a better alignment assessment.

The selecting solution that was found for this and several other landmarks is also a limitation as it makes finding the landmarks very user-dependent, as previously stated. More efficient solutions must be found, but they will surely require some deeper knowledge of Python.

As for the program testing, one of the biggest limitations was the dependency on other users to be able to have intraobserver results, both for the intraobserver reliability testing and the functionality testing. Performing only interobserver results would have been easier but it would pose as a source of false results, as, not only the same user is more likely to make the same mistakes over again, it would also cause more fatigue and this could induce errors. In this way, the intraobserver approach was preferred, but with the associated cost of a smaller sample size, which limits the scope of the analysis of the test results.

For better testing, more users need to be involved and more patients need to be evaluated, so that more comprehensive tests can be performed.

9. FUTURE WORK

As with any project, a lot can still be done and improved regarding the developed software and the ultimate goal of fully developing a preoperative planning method.

In the first place, it is necessary to focus some attention on the methods that calculate the torsion angles, as these are the main advantage of the 3D assessment, and therefore should be the primary focus of the software. The methods should be further analyzed and solutions should be found in order to make the measurement of these angles more reliable and precise.

Then, further extensive testing for clinical validation is necessary so that the software and the assessment method it provides can be validated and later incorporated in everyday practices of the *3D Chirurgie* group at the *Klinik für Allgemeine, Unfall- und Wiederherstellungschirurgie*. This testing phase is already planned and will be carried out by medical students of LMU.

Once this first version of the program has proved to be fully functional, the adaptation of the program by a more experienced programmer should take place, to allow for its use in a free platform instead of a paid platform like *Geomagic*. This will require extremely advanced 3D rendering and manipulation programming skills, but it will allow the program to run on any platform, which will mean less costs on software in the long run. This could also mean that there will be some needed improvement of the methods used to find the desired landmarks that were limited by the capabilities of *Geomagic*.

The plan is to also include a tool that allows the visualization of the surgical procedure and/or results of the surgery, which could even be used to give the surgeon some insight or even to show the patient what he will look like after the surgery. The program might even be used to develop cutting guides using 3D printing in order to facilitate de surgeon's work and also to ensure minimum human error, which is, after all, the point of the whole software.

10. CONCLUSION

Four different goals were set at the beginning of the project and, even with some limitations and required adaptations, all four of them were achieved: it was ensured that the needed 3D models can be generated by any user without great variability/error in the outcome, and therefore can be used for the alignment assessment; the exact angles and measures needed for a proper alignment were perfectly understood and the definition of the needed anatomic landmarks in order to calculate them came naturally; a program that uses the generated 3D models and returns all the needed angles and measures was successfully developed; and finally the program was put trough several test that not only show that the program is reliable and consistent in its results, but that it also poses as an improvement when compared to the manual assessment method.

As it was said before, this project comes from the will of the *3D Chirurgie* group to make use of new available technology and apply it to their practice of medicine, modernizing its planning methods. This combination of technology and medicine in order to give patients the best healthcare solution possible is the exact purpose of Biomedical Engineering and so, being at the heart of such project, particularly at the end of my academic path, was of great honor to me. Hopefully, the project can keep on evolving and ultimately be used to perform the preoperative planning of deformity correction and knee surgery, not only in Munich, but all over the world.

REFERENCES

(1) VanPutte, C. L., & Seeley, R. R., *Seeley's anatomy & physiology,* New York: McGraw-Hill, pp. 238-243, 2014

(2) Gilroy, A. M., MacPherson, B. R., Ross, L. M., Schünke, M., Schulte, E., & Schumacher, U, *Atlas of anatomy*, New York: Thieme, pp. 360-362, 2014.

(3) Feldman, D. S., *Lower Limb Deformities*. [Online] Available at: davidsfeldmanmd.com/specialties/lower-limb-deformities.

(4) Paley, D., *Principles of Deformity Correction,* Berlin: Springer Berlin Heidelberg, pp. 2429-2489, 2002.

(5) N. Awang, R. Sulaiman, A. Shapi'i, A. H. A. Rashid, M. F. M. Amran, and S. Osman, "A comparative study of computer aided system Preoperative planning for high Tibial Osteotomy," in Lecture Notes in Computer Science. Springer Nature, pp. 189–198, 2015.

(6) M. Viceconti et al., "CT-based surgical planning software improves the accuracy of total hip replacement preoperative planning", Medical Engineering & Physics, vol. 25, no. 5, pp. 371–377, 2003.

(7) S. Utzschneider et al., "Development and validation of a new method for the radiologic measurement of the Tibial slope", Knee Surgery, Sports Traumatology, Arthroscopy, vol. 19, no. 10, pp. 1643–1648, 2011.

(8) F. M. Buck, R. Guggenberger, P. P. Koch, and C. W. A. Pfirrmann, "Femoral and Tibial torsion measurements with 3D models based on low-dose Biplanar Radiographs in comparison with standard CT measurements", American Journal of Roentgenology, vol. 199, no. 5, pp. W607–W612, 2012.

(9) W. Yang, Q. Xing, J. Li, M. M. Theiss, Q. Peng, and J. X. Chen, "Automatic assessment of the torsional alignment of the knee joint in three-dimension visualization", Proceedings of the 9th ACM SIGGRAPH Conference on Virtual-Reality Continuum and its Applications in Industry - VRCAI '10, 2010.

(10) H. Kawakami et al., "Effects of rotation on measurement of lower limb alignment for knee osteotomy", Journal of Orthopaedic Research, vol. 22, no. 6, pp. 1248–1253, 2004.

(11) B. S. Kyung et al., "Are navigation systems accurate enough to predict the correction angle during high Tibial Osteotomy? Comparison of navigation systems with 3-Dimensional computed tomography and standing Radiographs", The American Journal of Sports Medicine, vol. 41, no. 10, pp. 2368–2374, 2013.

(12) A. Perlich, B. Preim, M. de La Simone, C. Gomes, E. Stindel, and A. Presedo, "Computer-aided surgery planning for lower limb Osteotomy", Bildverarbeitung für die Medizin 2011, Springer Nature, pp. 194–198, 2011.

(13) K. Subburaj, B. Ravi, and M. Agarwal, "Computer-aided methods for assessing lower limb deformities in orthopaedic surgery planning", Computerized Medical Imaging and Graphics, vol. 34, no. 4, pp. 277–288, 2010.

(14) A. B. Rosskopf, C. W. A. Pfirrmann, and F. M. Buck, "Assessment of two-dimensional (2D) and three-dimensional (3D) lower limb measurements in adults: Comparison of micro-dose and low-dose biplanar radiographs", European Radiology, vol. 26, no. 9, pp. 3054–3062, 2016.
(15) T. Illés and S. Somoskeöy, "The EOS™ imaging system and its uses in daily orthopaedic practice", International Orthopaedics (SICOT), vol. 36, no. 7, pp. 1325–1331, 2012.
(16) P. Thelen, C. Delin, D. Folinais, and C. Radier, "Evaluation of a new low-dose biplanar system to assess lower-limb alignment in 3D: A phantom study", Skeletal Radiology, vol. 41, no. 10, pp. 1287–1293, 2012.
(17) Cooke, D., Sled, E. u. Scudamore, A., "Frontal plane knee alignment: a call for standardized measurement", The Journal of Rheumatology 34, S. pp. 1796– 1801, 2007.
(18) Hernandez, R., Tachdjian, M., Poznanski, A. and Dias, L., "CT determination of femoral torsion", American Journal of Roentgenology, 137(1), pp. 97-101, 1981.
(19) Strecker, W., Keppler, P., Gebhard, F. u. Kinzl, L., "Length and torsion of the lower limb", The Journal of Bone and Joint Surgery 79, pp. 1019–1023 , 1979.
(20) Sayli, U., Bölükbasi, S., Atik, O.S., Gündogdu, S., "Determination of Tibial torsion by computed tomography", J Foot Ankle Surg, 33(2), pp. 144-7, 1994.
(21) Victor, J., Van Doninck, D., Labey, L., Innocenti, B., Parizel, P. and Bellemans, J., "How precise can bony landmarks be determined on a CT scan of the knee?", The Knee, 16(5), pp.358-365, 2009.
(22) Gwet, K., *Handbook of Inter-Rater Reliability: The Definitive Guide to Measuring the Extent of Agreement Among Multiple Raters*, Advanced Analytics, LLC, Maryland, USA, 2012

FIGURES

(A) Drake, R., Vogl, W., Mitchell, A. and Gray, H., *Gray's anatomy for students,* 2nd ed. Philadelphia, PA: Churchill Livingstone/Elsevier, 2012
(B) C. Uquillas, W. Rossy, C. K. Nathasingh, E. Strauss, L. Jazrawi, and G. Gonzalez-Lomas, "Osteotomies about the knee", The Journal of Bone and Joint Surgery-American Volume, vol. 96, no. 24, pp. e199–1–8, 2014.
(C) Q. Xing, W. Yang, M. M. Theiss, J. Li, Q. Peng, and J. X. Chen, "3D automatic feature construction system for lower limb alignment", 2010 International Conference on Cyberworlds, 2010.
(D) *Corrective osteotomy* [Online]. Available at: http://kneehipspine.com/subtopic/corrective-osteotomy/9.
(E) Paley, D., *Principles of Deformity Correction,* Berlin: Springer Berlin Heidelberg, pp. 2442, 2002.
(F) Paley, D., Tetsworth, K., "Mechanical Axis Deviation of the Lower Limbs", Clinic Orthopaedics and Related Research, no. 280, pp. 48-64, 1992.
(G) Victor, J., Van Doninck, D., Labey, L., Innocenti, B., Parizel, P. and Bellemans, J., "How precise can bony landmarks be determined on a CT scan of the knee?", The Knee, 16(5), pp.358-365, 2009.